

PYROLYSIS OF PHENOLIC RESIN IN SIC

BY

KEVIN KEEFE

A THESIS
SUBMITTED TO THE FACULTY OF

ALFRED UNIVERSITY

IN PARTIAL FULFILLMENT OF THE REQUIREMENTS
FOR THE DEGREE OF

MASTER OF SCIENCE

IN

CERAMIC ENGINEERING

ALFRED, NEW YORK

SEPTEMBER, 2015

Alfred University theses are copyright protected and may be used for education or personal research only. Reproduction or distribution in part or whole is prohibited without written permission from the author.

Signature page may be viewed at Scholes Library, New York State College of Ceramics, Alfred University, Alfred, New York.

PYROLYSIS OF PHENOLIC RESIN IN SIC

BY

KEVIN KEEFE

B.S. Alfred University (2013)

SIGNATURE OF AUTHOR _____

APPROVED BY _____

William Carty, ADVISOR

Matthew Hall, ADVISORY COMMITTEE

Andrew Eklund, ADVISORY COMMITTEE

CHAIR, ORAL THESIS DEFENSE

ACCEPTED BY _____

DOREEN D. EDWARDS, DEAN
KAZUO INAMORI SCHOOL OF ENGINEERING

ACKNOWLEDGEMENTS

This work could not have been completed without the help and support of many people and for that I thank you all sincerely. My committee, Nikolas Ninos, Calix Ceramic Solutions, the CACT office at AU and Exothermics thank you for the support and guidance. Dave Crenshaw, Fran Williams, Gerry Wynick and Jim Thiebaud thank you for the technical support. Krishna, for being wonderful and extremely helpful! Everyone else: Diana, Tom and Tom Clifton Keefe, Monica, Jim and Alex Fredell and all of my family, friends and of course the office group, thank you for the support.

Dr. William Carty, my friend and advisor, deserves special recognition. His support and guidance over the last six years has facilitated my growth both personally and professionally. He has a candid ability to oversee your work, add meaningful insight and direction, thoroughly confuse you and lead you out of the rabbit hole all while talking about mullite at Alex's over a Harvest. I cannot forget to mention his talent of editing and the mental side effects it has on his advisees. Although difficult, the forest is always seen through the trees and it has made anyone who experiences it a better writer. Recognition has to be given to Ani and the rest of his family. After Ana and I were considered "Stella approved", a wonderful friendship was built. I am grateful to have had the chance to work with and befriend you, what a long strange trip it's been Bill.

Anyone who has worked with Dr. Carty knows that the real power is with Hyojin Lee. With countless students, projects and problems, Hyojin always made time for me and I thank him for that. A true friend at heart, Hyojin and his family has always treated me as such; they even hosted a birthday party for me.

Nikolas Ninos, this work most certainly could not have been done without you. From the funding for the project to the brainstorming and observations we've had along the way, thank you. I hope this work helps you in your SiC endeavors.

Anastasia Fredell, where do I begin? Thank you for your love and support thought this journey. I can honestly say that without you I could not have made it to this point and for that I am indebted. You have always believed in me, arguably even when you shouldn't have and that has made all the difference. Thank you Ana, now we can move on with our lives!

TABLE OF CONTENTS

Acknowledgements.....	iii
Table of Contents.....	iv
List of Tables	vi
List of Figures.....	vii
Abstract.....	x
I. INTRODUCTION.....	1
A. Scope of Work	2
A.1 Hydrogen Stripping.....	2
II. LITERATURE REVIEW	5
A. Sintering of Silicon Carbide.....	5
B. Industry Standard (Conventional) Pyrolysis.....	5
C. Background of Phenolic Resin.....	6
C.1 Common Pyrolysis Conditions and RXN's	6
III. EXPERIMENTAL PROCEDURE.....	9
A. Thermogravimetric Analysis	9
B. Construction of Tube Furnaces and Gas Flow System.....	10
C. Pyrolysis Sample Preparation	11
D. Statistical Experimental Design (S.E.D.).....	12
E. Pyrolysis Runs	14
F. S.E.D. Responses	15
F.1 Weight Loss	15
F.2 LECO Carbon Analysis	15
F.3 Carbon Content via True Density.....	15
F.4 Sintering.....	17

F.4.1 Sintered Density.....	17
IV. RESULTS AND DISCUSSION	19
A. TGA Experiments	19
A.1 Standard Pyrolysis.....	20
A.2 SiC Granules	21
A.3 Paraffin + Alumina Surrogate	26
A.4 Phenolic + Alumina Pyrolysis	32
B. S.E.D. Experiments.....	42
B.1 Response: Sintered (Relative) Density.....	43
B.2 Response: Mass Loss	47
B.3 Response: LECO Carbon Analysis	48
B.4 Response: Carbon Content via True Density	50
B.5 Optimization.....	52
V. SUMMARY AND CONCLUSIONS	54
VI. FUTURE WORK.....	55
REFERENCES.....	56
APPENDIX.....	59
A. S.E.D. Data	59

LIST OF TABLES

Table I. Enthalpy of Formation (Δh_f) Data for Bonds of Interest ^{7,8,9,10}	2
Table II. TGA Operating Parameters.....	9
Table III. SiC Granule Composition.....	11
Table IV. Green Sample Puck Dimensional Statistics	12
Table V. S.E.D. Factors and Levels.....	12
Table VI. Raw Powder Chemistries. Calculated from True Density Measurements and the Rule of Mixtures.....	17
Table VII. Characteristic Temperatures for Pyrolysis in Nitrogen and Air	24
Table VIII. Average Relative Density and Standard Deviation	45
Table IX. S.E.D. Factor Labels and Names.....	43
Table X. ANOVA Results for Relative Density (2100°C) Response	45
Table XI. ANOVA Results for Mass Loss Response.....	47
Table XII. Starting SiC Powder Chemistry from LECO Oxygen Results	49
Table XIII. ANOVA Results for Carbon Content Response.....	50
Table xiv. Table of Optimization Parameters	53

LIST OF FIGURES

Figure 1. Ellingham diagram for oxides with CO, CO ₂ and H ₂ O region enlarged ¹²	4
Figure 2. Proposed repeat unit before and after hydrogen stripping	4
Figure 3. Schematic of a standard pyrolysis furnace cycle	5
Figure 4. Example of crosslinking via condensation reactions in phenolic resin ¹⁹ ...	7
Figure 5. Example of chain scission at methylene bridges ²	7
Figure 6. Example of polycyclic aromatization ²	7
Figure 7. Schematic of cured resol resin chain scission ¹	8
Figure 8. Gas flow system schematic	11
Figure 9. Design matrix	13
Figure 10. Pyrolysis profile schematic	14
Figure 11. Drilled sample cutting template	14
Figure 12. Schematic of TGA data.	19
Figure 13. TGA of standard pyrolysis cycle.....	20
Figure 14. Tga of SiC granules in air.....	21
Figure 15. TGA of SiC granules in nitrogen.	22
Figure 16. TGA of SiC granules in nitrogen and air	23
Figure 17. Extracted TGA data of SiC granules. Characteristic temperature as a function of heating rate.	24

Figure 18. Extracted TGA data of SiC granules: peak temperature mass loss as a function of heating rate.	25
Figure 19. TGA of paraffin + alumina in 21.5% O ₂	27
Figure 20. TGA of paraffin + alumina in 5% O ₂	28
Figure 21. TGA of paraffin + alumina air and 5% O ₂ comparison, 175°C dwell ..	29
Figure 22. Maximum carbon yield as a function of paraffin stoichiometry.....	30
Figure 23. Extracted TGA data of paraffin + alumina. Plot of % expected residue after the dwell temperature as a function of dwell temperature.	31
Figure 24. Extracted TGA data of paraffin + alumina.....	32
Figure 25. TGA of phenolic + alumina in 2% O ₂	33
Figure 26. Weight loss during the dwell period, in 2% O ₂	34
Figure 27. TGA of phenolic + alumina in 5% O ₂	35
Figure 28. Weight loss during the dwell period, in 5% O ₂	36
Figure 29. TGA of phenolic + alumina in air.	37
Figure 30. Weight loss during the dwell period, in air	38
Figure 31. TGA of phenolic + alumina comparison, 200°C dwell.	39
Figure 32. Weight loss during the dwell period, 200°C dwell temperature.	40
Figure 33. TGA residue data of phenolic + alumina, residue after dwell	41
Figure 34. TGA residue data of phenolic + alumina, residue after peak temperature	42

Figure 35. Density and porosity plot as a function of sintering temperature.	44
Figure 36. Contour plot for relative density (2100°C)	46
Figure 37. Micrographs of polished sintered samples	47
Figure 38. Contour plot for mass loss.....	48
Figure 39. Contour plot for carbon yield.	51
Figure 40. Contour plot of desirability for pyrolysis process optimization	52
Figure 41. Cube plot of desirability	53

ABSTRACT

When phenolic resin is pyrolyzed, carbon is left behind. Maximizing the carbon yield from this pyrolysis was the goal. Standard pyrolysis loses a sizeable amount of carbon in the form of volatile organic compounds (VOC's) due to polymer chain scission. It is proposed that by selectively stripping hydrogen from the polymer, carbon yield can be increased.

Pressureless sintering of silicon carbide (SiC) requires excess carbon for densification. Carbon can be introduced either by adding carbon or a carbonaceous polymer that will be pyrolyzed. The SiC production granules that were used contained phenolic resin. There are two purposes for the resin: first, when cured, the strength of the phenolic resin allows for green machining and second, providing excess carbon from pyrolysis.

To test if hydrogen can be preferentially removed to increase carbon yield, the pyrolysis conditions were changed. Thermogravimetric analysis (TGA) experiments were conducted to identify the heating rate and peak temperature along with the pyrolysis behavior in different gas chemistries and dwell temperatures. From industry, it was understood that flow rate has an impact on pyrolysis. A statistical experimental design was created to test flow rate (0, 7.5 and 15 ml/sec), gas chemistry (2%, 5% and 10% O₂, balance nitrogen) and dwell temperature (150°C, 200°C and 250°C). The pyrolyzed samples were sintered (below the optimal sintering temperature) to understand the effect that pyrolysis has on the sinterability on SiC.

TGA demonstrates that a higher carbon yield is seen with lower dwell temperatures and increased oxygen levels. All samples fully densified at 2100°C. Flow rate was found to be statistically significant in increasing carbon yield from pyrolysis. The measured carbon yields were not greater than those obtained from the standard pyrolysis used in industry. However, the standard pyrolysis stops at 600°C and the TGA data suggests that the pyrolysis is not complete. The TGA data suggests that the hydrogen stripping hypothesis has merit.

I. INTRODUCTION

Phenolic resin is a polymeric additive that is used in the processing of pressureless sintered silicon carbide (SiC). In the application of this work, phenolic resin is used for two reasons: first, as a binder that will increase green strength and second, as a carbon source once pyrolyzed. It is proposed that the efficiency of the carbon yield can be increased by selectively stripping hydrogen from the polymer during pyrolysis.

Silicon carbide is difficult to sinter without additives or being assisted by pressure. Having free carbon in the microstructure reduces the oxide layer (silica) that exists on the surface of the SiC particles. By cleaning the particle surface along with the introduction of boron, SiC can be directly sintered.

The standard production pyrolysis cycle uses a nitrogen atmosphere and a dwell temperature of 400°C. The carbon yields are approximately 23.5 wt. % of expected carbon. During pyrolysis, the polymer chain is cut via chain scission reactions and results in organic compounds becoming volatile. These volatile hydrocarbons remove potential free carbon from the system, driving down the carbon yield efficiency. By stripping the hydrogen from the polymer before this scission, the polymer network will be strengthened and carbon yield could increase.

To test this hypothesis, a series of TGA experiments were conducted to establish the optimal heating rate and peak temperature, the materials baseline behavior and the effect of gas chemistry and dwell temperature on pyrolysis. With the TGA results, a statistical experimental matrix was created to test flow rate, atmosphere (oxygen level) and dwell temperature. Carbon yield, weight loss and sintered density were the responses to the experiments.

The TGA data suggests that hydrogen stripping is working. Low dwell temperatures and the incorporation of oxygen showed higher yields. The statistical experimental design (S.E.D.) results show that flow rate was a statistically significant variable; high flow rates resulted in high yields. The carbon yield from the standard pyrolysis was higher than that of all the tested samples. However, the data suggests that the mass loss of the standard pyrolysis cycle is not complete at the temperature used.

Conventional pyrolysis conditions for carbon retention were challenged. According to literature, the approach is unique. The goal was to maximize the residual (free) carbon from pyrolysis by selectively stripping hydrogen from the polymer structure.

A. Scope of Work

This work was performed to optimize the carbon yield of the resin in SiC. Pyrolysis thermolytically breaks bonds of the polymerized chain to yield amorphous carbon. Conventional pyrolysis of this system is performed in a flowing non-oxidative atmosphere (nitrogen) that is heated to an intermediate temperature and then further heated to a peak temperature.

The problem with conventional pyrolysis is that a lot of carbon is lost with the volatile products of the process. Literature indicated that pyrolysis products with a molecular weight less than 125 g/mol will be volatile during pyrolysis.^{1,2,3,4,5,6} Increasing the temperature may increase the molecular weight cutoff likewise, decreasing the temperature may decrease the cutoff.

The idea behind the hypothesis was being able to selectively strip hydrogen atoms from the polymer structure. Stripping the hydrogen forces carbon double bonds to form on the benzene ring, further stabilizing the polymer structure. This could lead to less carbon being removed in the form of volatile, high molecular weight hydrocarbons.

A.1 Hydrogen Stripping

In researching the bond dissociation energies of hydrocarbons, it was found to be extremely difficult to try to predict what bonds would break under certain conditions and their sequence. The data in Table I are known enthalpies of formation of certain bonds of interest (they are expected to be present in the phenolic resin structure). The data shows that methylene scission is a favored reaction (Phenol-Toluene data). The only reactions more favorable are the removal of the hydroxyl group on a chain termination molecule and the breaking of a H-C bond. The H-C bond is present in the structure however; it is in the form of more complex carbon compounds.

Table I. Enthalpy of Formation (ΔH_f) Data for Bonds of Interest^{7,8,9,10}

Compound	Bond to Break	ΔH_f (kJ/mol)
Hydroxyl-Toluene	HO-C ₆ H ₅ CH ₃	322

Hydrogen-Carbon	H-C	337.2
Phenol-Toluene	HOH ₅ C ₆ -CH ₂ C ₆ H ₅	347
Hydroxyl-Benzyl	HO-C ₆ H ₅ CH ₂	353.55
Hydrogen-Phenol	H-OC ₆ H ₅	368
Hydrogen-Benzyl	H-C ₆ H ₅ CH ₂	375.72
Hydrogen-Benzene	H-C ₆ H ₅	431

It is important to note that there was no data found for removing a hydrogen atom from the cresol structure (HO-C₆H₅-CH₂). It is known that the addition of functional groups to the benzene ring will reduce ΔH_f of the subsequent molecules.⁷ This is seen in the last two entries of Table I: $\Delta H_{f, \text{H-Benzene}} > \Delta H_{f, \text{H-Benzyl}}$. Therefore, it is assumed that $\Delta H_{f, \text{H-Benzyl}} > \Delta H_{f, \text{H-Cresol}}$, meaning that it is predicted that stripping hydrogen from the cresol backbone structure will be thermodynamically favored over stripping it from the benzyl molecule.

Recent binder burnout research shows that a dirty burnout can be obtained from pyrolyzing in a slightly oxidative environment.¹¹ This implies that there are oxidative and thermal contributions to bond breakage (when in the presence of oxygen), rather than just a thermolytic contribution. This is seen in the oxide stability diagram, also known as the Ellingham diagram (Figure 1). In this diagram, Gibb's free energy (ΔG°) is plotted versus temperature. It shows oxide stability as a function of temperature and environment. Of interest in this diagram are the lines labeled 1, 2 and 3. Line 1 is the 2CO₂ line from the reaction of 2CO and O₂. Line 2 is 2H₂O from the reaction of 2H₂ and O₂, and line 3 is CO₂ from the reaction of C and O₂. It is seen at 850°C that line 3 is most favorable. At approximately 675°C line 1 is most favorable. At about 525°C, line 1 is most favorable however, there is no CO present in the material therefore, line 2 is favorable. What this shows is that if given the chance to react with either carbon or hydrogen, oxygen gas will prefer to react with hydrogen to form water up until about 525°C.

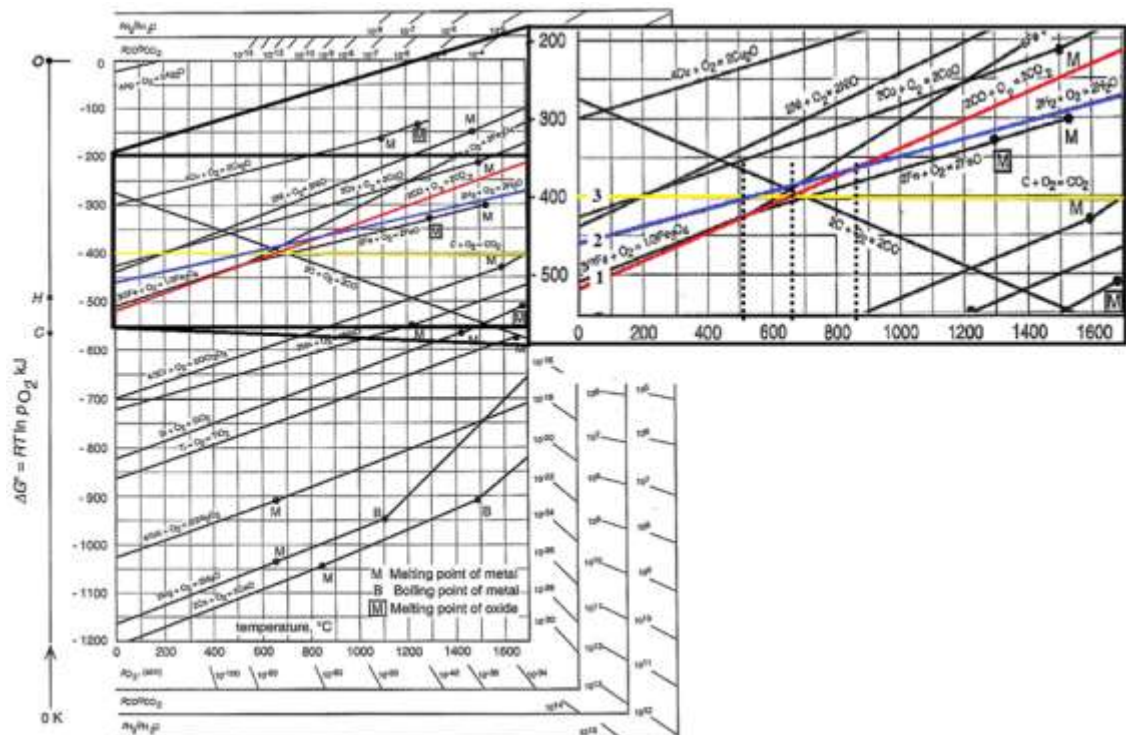


Figure 1. Ellingham diagram for oxides with CO, CO₂ and H₂O region enlarged¹²

Combining the thermodynamic data, the binder burnout research and the data from the Ellingham diagram, the hypothesis of hydrogen stripping was established. The idea is that by firing in a slightly oxidative environment, hydrogen atoms will be preferentially stripped from the polymer structure, combine with O₂ to form H₂O and force carbon to form double bonds in the benzene ring. This will produce a stronger, more stable structure that will inhibit the methylene bridge scission and increase the carbon yield from pyrolysis. Figure 2 is the proposed repeat unit before and after hydrogen stripping.

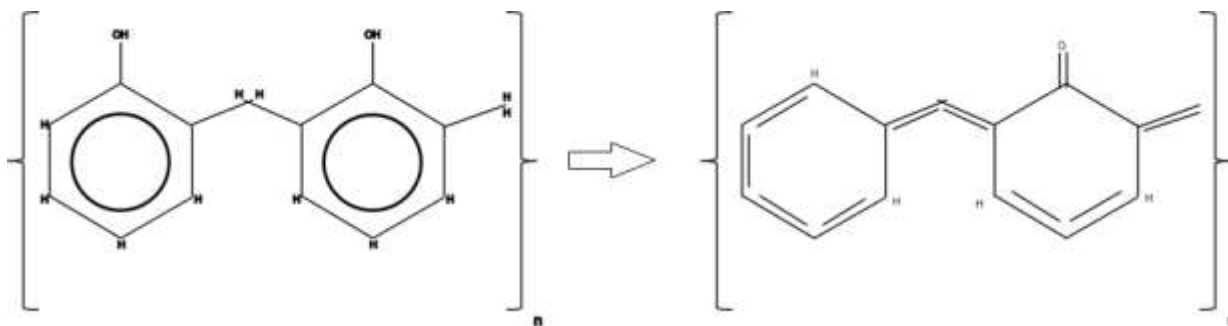


Figure 2. Proposed repeat unit before and after hydrogen stripping

II. LITERATURE REVIEW

A. Sintering of Silicon Carbide

Silicon carbide is difficult to densify via solid state sintering. This difficulty is credited to the high grain boundary to surface energy ratio.^{13,14,15} It has been shown that boron can reduce γ_{GB} by becoming segregated in the grain boundaries however, it is not enough to allow sintering to occur.¹⁴ It is also known that SiC powders can have oxide surface layers (SiO_2) formed from SiC oxidation. By introducing carbon, the silica surface layer is reduced via carbothermic reduction starting at 1200°C.

Cleaning the surface of SiC particles increases the surface energy.¹⁴ With boron lowering the grain boundary energy and carbon increasing surface energy, the ratio is reduced and pressureless sintering of SiC is attainable.

B. Industry Standard (Conventional) Pyrolysis

Conventional pyrolysis of phenolic resin is performed in a nitrogen atmosphere. While some literature indicates a constant heating rate to a peak temperature, the industrial pyrolysis of phenolic resin utilizes multiple heating rates and dwells at both the intermediate and peak temperature.¹⁶ Figure 3 is a schematic of a standard pyrolysis furnace cycle.

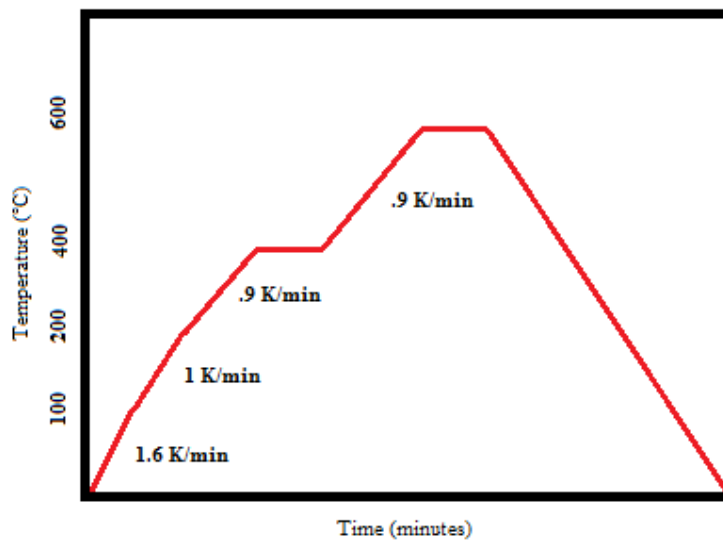


Figure 3. Schematic of a standard pyrolysis furnace cycle

The heating rate varies from 0.9-1.6 K/min, a dwell temperature of 400°C for 120 minutes, a peak temperature of 600°C (with a 120 minute dwell) and flow rates near 5 SLM (standard liters per minute).

C. Background of Phenolic Resin

Phenolic resin is a synthetic polymer that has useful applications in a number of applications including: molding compounds, wood working, abrasives, adhesives and ceramic powder processing.¹⁷ This synthetic polymer consists mainly of two constituents: phenol and formaldehyde that react to form the polymer. There are three main reaction categories in phenol formaldehyde resin: formaldehyde addition to phenol, chain growth and crosslinking (curing) reactions.^{1,2,17,18,19,20,21} Changing the temperature and pH under which phenol reacts with formaldehyde will change the polymer structure.¹⁷ There are two types of commercially available phenol formaldehyde resins: Resol and Novolak. The conditions of the formaldehyde addition reaction will determine whether a resol or novolak resin is formed.

A novolak resin is formed when formaldehyde and phenol react in a strongly acidic pH region.¹⁷ They are considered to be mainly linear polymers linked with methylene bridges. Novolaks are considered “two-step” resins because of the addition of a curing agent like hexamethylenetetramine (HMTA).¹⁷ Novolak resins are soluble, thermoplastic and have low molecular weights up to 2000 g/mol.¹⁷

Resol resins are formed when phenol and (excess) formaldehyde react under alkaline conditions.¹⁷ This reaction yields mono or polynuclear hydroxymethylphenols (HMP). HMP is cross-linked (cured) by the addition of heat and sometimes acids. Once cured, a stable three dimensional, insoluble, infusible polymer network is formed with an undetermined molecular weight.¹⁷ The resin used in this thesis is a resol resin.

C.1 Common Pyrolysis Conditions and RXN's

It is commonly understood that the thermal degradation of phenolic resins occurs in three stages: 1) crosslinking via condensation reactions, 2) chain scission at methylene bridges and 3)

hydrogen removal via polycyclic aromatization.^{1,2,17,18,19,20,21} Figures 4, 5 and 6 schematically show some of the reactions happening in these stages.

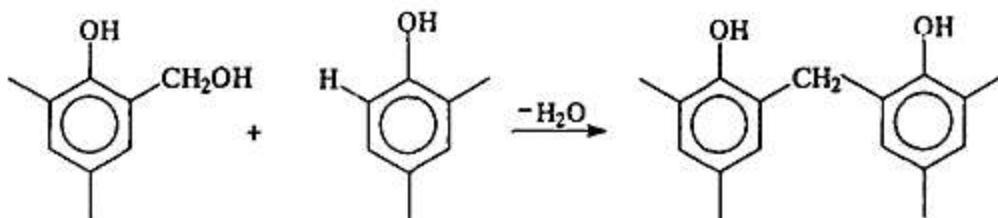


Figure 4. Example of crosslinking via condensation reactions in phenolic resin¹⁹

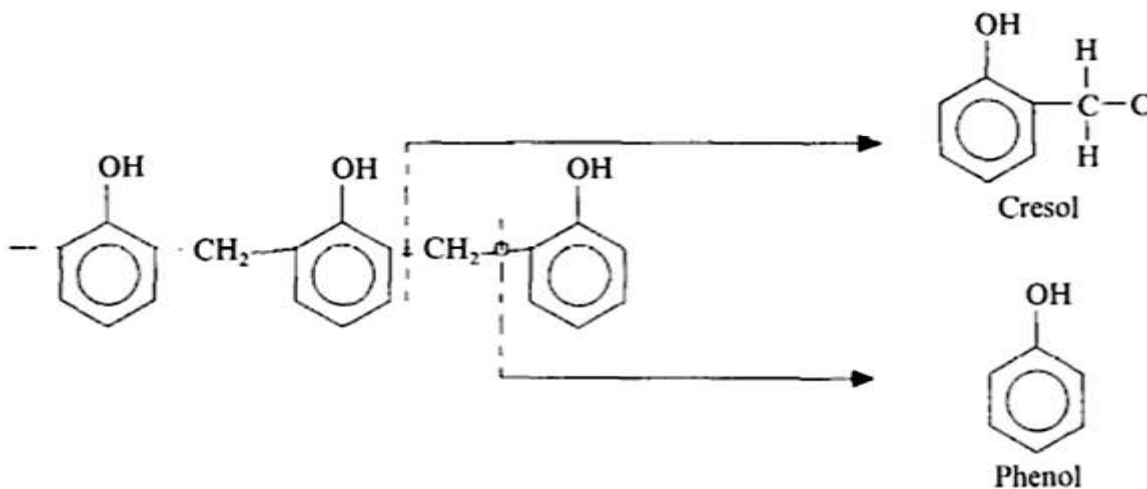


Figure 5. Example of chain scission at methylene bridges²

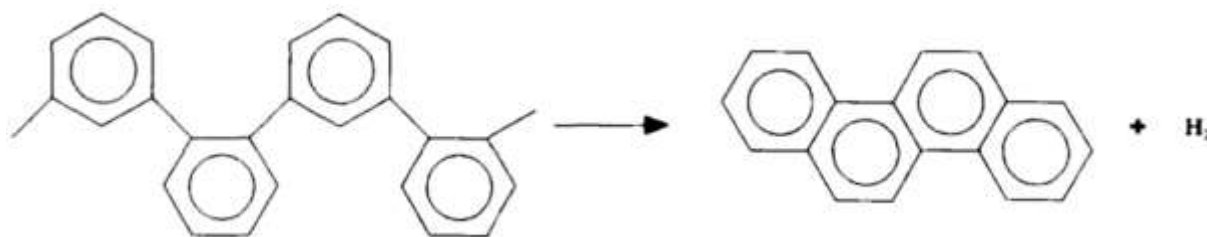


Figure 6. Example of polycyclic aromatization²

Methylene scission controls the polymer degradation. It is known that not all methylene bridges are broken, hence the structure in Figure 5, however the degree of depolymerization via scission influences the carbon yield of the polymer.^{3,22} By increasing the degree of depolymerization, the carbon yield decreases.

The structure of phenolic resin is very complex. Figures 4-6 are the most widely accepted degradation methods to describe those regions however, other reactions occur in parallel. Figure 7 represents a cured resol resin and the results of chain scission. The approach of this project was to try to bypass the chain scission, strengthen the polymer structure to reduce VOC's and in turn increase carbon retention.

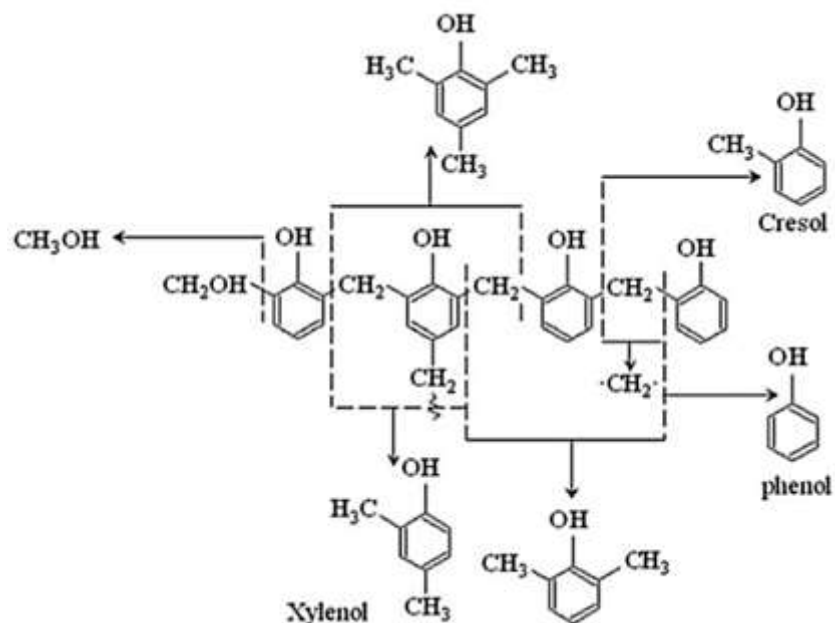


Figure 7. Schematic of cured resol resin chain scission¹

III. EXPERIMENTAL PROCEDURE

A. Thermogravimetric Analysis

Thermogravimetric analysis (TGA) (SDT Q600, TA Instruments, USA) experiments were used to evaluate weight loss with varying pyrolysis conditions to determine the conditions for the S.E.D. TGA experiments consisted of four subjects: 1) standard pyrolysis, 2) SiC granules for heating rate determination, 3) paraffin pyrolysis surrogate and 4) phenolic resin with alumina pyrolysis. Table II shows the operating parameters for the different subjects. All testing gasses used were mixtures of oxygen and nitrogen. The phenolic + alumina samples had the mixed gas flowed through the dwell period; nitrogen was used for the remainder of the run. All TGA experiments had a 60 minute dwell period, where applicable. Dried A-10 alumina powder was used as the reference material and platinum pans were used in all TGA experiments.

Table II. TGA Operating Parameters

	<i>Standard Pyrolysis</i>	<i>SiC Granules</i>	<i>Paraffin + Alumina Surrogate</i>	<i>Phenolic Resin + Alumina</i>
Heating Rate K/min	0.9-1.6	2,5,10,20	10	10
Dwell (Y/N) (60 minutes)	Y	N	Y	Y
Intermediate Dwell Temperature (°C)	400	-	150-220	200-300
Peak Temperature (°C)	600	900	900	900
Atmosphere	Nitrogen	Nitrogen, 21.5% O ₂	Nitrogen, 2% O ₂ , 5% O ₂ , 21.5% O ₂	Nitrogen, 2% O ₂ , 5% O ₂ , 21.5% O ₂
Atmosphere Post- Dwell	Nitrogen	-	Nitrogen	Nitrogen

50mg samples were targeted for all TGA experiments. The premixed SiC granules were pyrolyzed using the standard pyrolysis parameters from industry practice. These granules were used for the heating rate determination experiments as well.

For the paraffin and phenolic experiments, 5 mg of either paraffin wax or phenolic resin was weighed into a platinum crucible, dried A-10 was then weighed and placed on top so the mass of the polymers would not exceed 10 wt% of the sample. Phenolic resin was dried at 120°C overnight, cured at 175°C overnight and then crushed into a powder using an automated mortar and pestle. The alumina was used to prevent bumping. It was assumed that there was no catalytic activity from the surface area of the alumina. The alumina had a surface area of approximately 1 m²/g.

B. Construction of Tube Furnaces and Gas Flow System

A custom gas flow system was designed and built that serviced two tube furnaces. The furnaces are identical wire kanthal element furnaces, modified to accept a high alumina tube. The gas flow system was designed to be controlled by a LabView application (LabView v. 2014, National Instruments, Austin TX). This system consisted of having two gas cylinder hookups and four mass flow controllers. With a series of check and solenoid valves, both gases can be controlled independently and service both furnaces simultaneously. A bubbler and trap were added downstream from the furnace to create an airlock and prevent flooding on cooling. This system can accurately control the flow rates of two gasses and the furnaces. It also has the ability to pulse gasses to approximate a “zero flow rate” condition. Figure 8 shows a schematic of the gas flow system. The two furnaces were tested and showed identical behavior during pyrolysis.

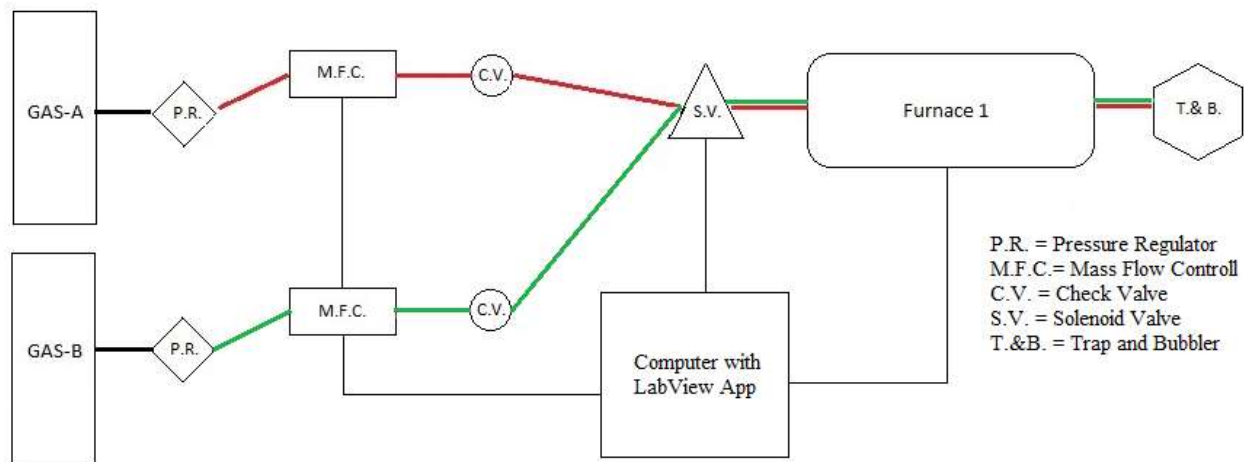


Figure 8. Gas flow system schematic

C. Pyrolysis Sample Preparation

The samples used in the experimental matrix were prepared from a pre-mixed, pre-granulated (spray dried) silicon carbide composition. Table III shows the composition of the granules.

Table III. SiC Granule Composition

Description	Material	Percentage (wt %)
Silicon carbide	SiC	86.96
Boron Carbide	B ₄ C	0.87
Binder	Phenolic Resin	6.09
Plasticizer	Polyvinyl Alcohol	3.47
Acrylic Binder	Rhoplex	2.61

The granules were uniaxially pressed in a hydraulic press (MD80, Aeonic Press Co., Easton, PA). 120 disks were pressed to 18 ksi; dimensions are shown in Table IV

Table IV. Green Sample Puck Dimensional Statistics

	Diameter cm (in)	Thickness cm (in)	Mass (g)
<i>Average</i>	5.94 (2.345)	1.19 (0.47)	61.62
<i>Standard Deviation</i>	0.003 (0.001)	0.03 (0.01)	0.65

The sample pucks were heat treated at 175°C to cure the resin in preparation for pyrolysis. Once cured, half of the samples were drilled in the center using a ¼” diamond drill bit to a depth of ¼”. This was used to set a thermocouple into the sample. Dimensions were measured and masses weighed, after curing and drilling.

D. Statistical Experimental Design (S.E.D.)

Based on the TGA results, an experimental matrix was designed to test pyrolysis conditions (Design Expert v9, Stat-Ease, Minneapolis, MN). A response surface design was chosen to allow optimization experiments. Due to using parameters that are not currently in practice, a Box Behnken design type was used. The advantage of using a Box Behnken design is that it can establish experimental boundaries and test within them for optimization. A design model that predicted the variables and their first order interactions was chosen.

From the TGA experiments the peak temperature and heating rate were determined and kept as constants. These experiments also helped to establish the tested ranges for dwell temperature and atmosphere. The S.E.D. was designed with the factors and factor levels shown in Table V.

Table V. S.E.D. Factors and Levels

Factor	Low Level	High Level
<i>Flow Rate (ml/sec)</i>	0	15
<i>Atmosphere (% O₂)</i>	2	10

<i>Dwell Temperature (°C)</i>	150	250
-------------------------------	-----	-----

The design resulted in 5 center points, 6 lack-of-fit runs and 7 experimental runs totaling 17 experiments (see Figure 9). The original responses included LECO carbon analysis, weight loss and sintered density. The experiments were organized in order of gas type, because of the nature of the gas flow system servicing both furnaces (i.e. both furnaces running 10% O₂).

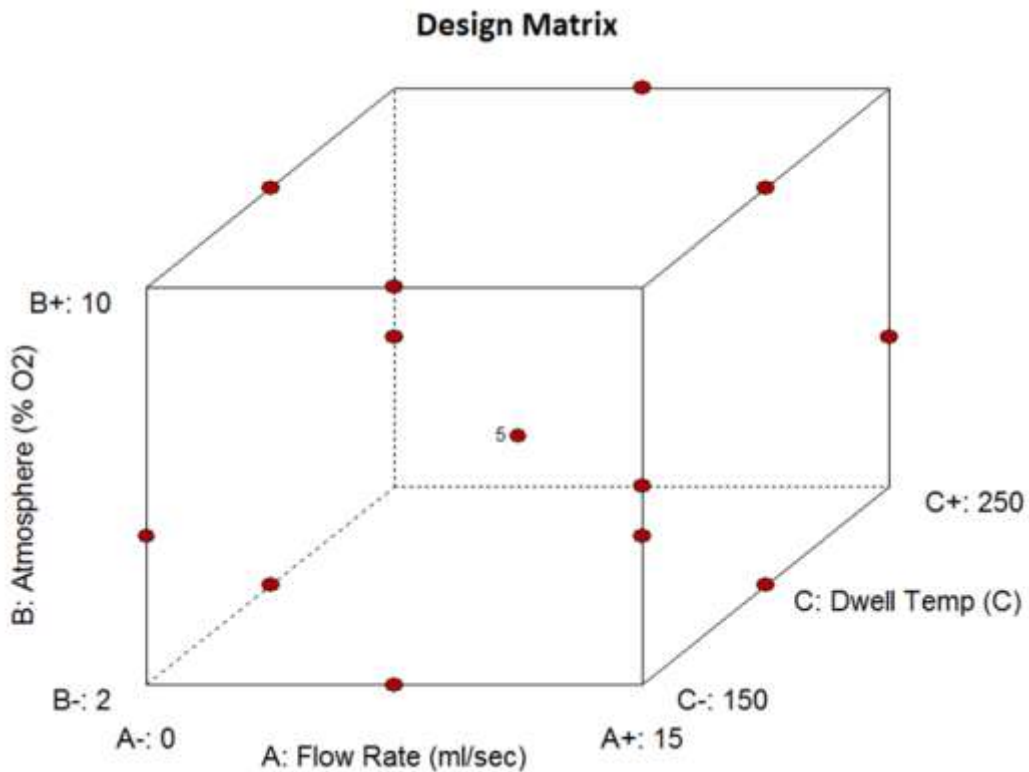


Figure 9. Design matrix

Figure 10 is a schematic of a typical pyrolysis profile used in the S.E.D. In Region I, an oxygen/nitrogen gas mixture was used. In Region II, only nitrogen gas was utilized.

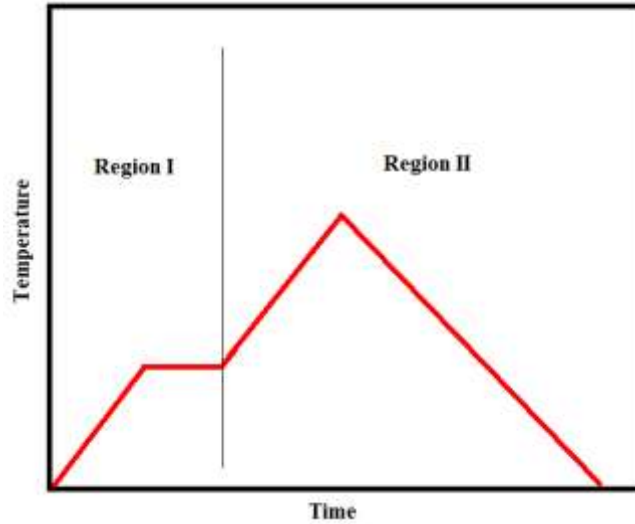


Figure 10. Pyrolysis profile schematic

E. Pyrolysis Runs

Two samples were used for each run: one was drilled for the thermocouple and the other was kept intact. The drilled samples were equipped with two thermocouples, one inside of the hole (with the sample inverted onto the thermocouple) and the other sitting on top of the sample. Each run included a 5 minute pre-cycle nitrogen purge and a nitrogen cooling purge. Once the runs were completed, dimensional measurements were taken.

After pyrolysis, each drilled sample was cut according to the template shown in Figure 11. The sections of the sample were utilized for different tests, as labeled. Each cut piece was labeled, cleaned with de-ionized water and dried overnight.

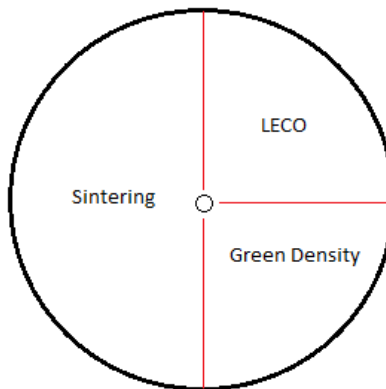


Figure 11. Drilled sample cutting template

F. S.E.D. Responses

F.1 Weight Loss

The mass of the sample pucks were weighed after pyrolysis. Weight loss was calculated from this measurement with the following equation.

$$\text{Weight loss (\%)} = \frac{(M_{\text{Cured}} - M_{\text{Pyrolyzed}})}{M_{\text{Cured}}} \times 100 \quad (1)$$

Where:

M_{Cured} = Mass of cured sample

$M_{\text{Pyrolyzed}}$ = Mass of pyrolyzed sample

F.2 LECO Carbon Analysis

Free-inorganic LECO carbon analysis is used to quantify the free carbon content (not chemically bound to Si) in the samples. The pyrolyzed samples were ground to a powder and sent to out for carbon analysis (Acme Analytical Labs, British Columbia, Canada). For inorganic testing, a 15% perchloric acid leach is done to remove any organic carbon. An induction furnace heated the sample to 1000°C using O₂ as a carrier gas.²³ The assumption behind the analysis is that any free carbon will react with oxygen to form CO₂.²³ The gas passes through an IR absorption cell that measures CO₂ level.²³ Results are reported as wt% CO₂, the detection limits are 0.02% (wt %).

F.3 Carbon Content via True Density

In a binary system (current samples: SiC+B₄C), mineralogy can be determined from the true density.²⁴ A helium pycnometer was used to measure the true density of the pyrolyzed samples.

The ground LECO samples were dried and measured. The bulk densities of the raw SiC and B₄C were also measured. It is understood that there is free carbon introduced from the starting

SiC and B₄C materials. These constituents were batched at a constant ratio allowing a “carbide density” to be calculated, measured and used as one of the mineralogical phases in the system.

The other phase was the carbon created by the pyrolysis of the resin. To account for this, phenolic resin was pyrolyzed without a powder bed. The bulk density of the remaining carbon was measured and used in the rule of mixtures calculations, Equation 2. The equation as shown, yields volume percent, a conversion to weight percent is necessary. This method allows the concentration of free carbon from pyrolysis to be calculated.

$$\rho_{sample} = (f_{v,carbide(SiC+B_4C)} \times \rho_{carbide}) + (f_{v,carbon} \times \rho_{carbon}) \quad (2)$$

Where:

$f_{carbide}$ = volume fraction of carbide

f_{carbon} = volume fraction of carbon

$\rho_{carbide(SiC+B_4C)}$ = density of carbide

ρ_{carbon} = density of carbon

The starting raw materials were measured and the free carbon contents were calculated. This allowed for the free carbon brought in with these materials to be accounted for in the calculations for free carbon from pyrolysis. Table VI shows the results of these measurements and calculations. For the SiC powder, the amount of silica present needed to be established so that an accurate amount of free carbon in the powder could be calculated (see B.4 in the Results section). For this calculation, since the given silica content is in wt. %, reciprocal density values were used in Equation 2 to calculate a wt. %. The “carbide” powder in Table VI is the blend of SiC and B₄C used in the granules. Of particular interest is the weight percent free carbon in the carbide powder, 1.39 wt. %. This shows that there is a significant amount of carbon introduced in the starting material.

Table VI. Raw Powder Chemistries. Calculated from True Density Measurements and the Rule of Mixtures

<i>SiC Powder</i>				
<i>Material</i>	<i>Measured Composite Density (g.cm⁻³)</i>	<i>Density (g.cm⁻³)</i>	<i>Percentage (v/o %)</i>	<i>Percentage (wt. %)</i>
SiC	3.1569	3.21	96	97.61
C*		1.706	2.53	1.36
SiO ₂		2.2	1.48	1.03
<i>B₄C Powder</i>				
B ₄ C	2.4669	2.52	93.48	95.49
C*		1.706	6.52	4.51
<i>“Carbide” Powder (SiC + B₄C)</i>				
SiC*	3.151	3.21	94.93	96.76
B ₄ C*		2.52	1.04	0.83
C*		1.706	2.57	1.39
SiO ₂		2.2	1.46	1.02

* denotes a measured density, not theoretical.

F.4 Sintering

All samples were sent out for sintering (Exothermics Inc., Amherst, NH) in a vacuum graphite furnace (Model 121224 G, Thermal Technologies, Santa Rosa, CA). The samples were intentionally underfired to try to expose sintering differences as a function of the pyrolysis conditions. Standard sintering temperature for this material is 2165°C. The first set of samples was sintered to 2000°C, 2050°C and 2100°C.

F.4.1 Sintered Density

Sintered density was measured using an immersion technique in deionized water.²⁵ The uncut pucks were broken and three pieces per sample were used for statistical significance. Apparent specific gravity was calculated from the measurements (Equation 3). Relative density was calculated from the apparent specific gravity (Equation 4).

$$\text{Apparent Bulk Density} = \frac{M_D}{(M_{SAT} - M_{SUSP})} \quad (3)$$

Where:

M_D = Mass of dried sample

M_{SAT} = Mass of saturated sample

M_{SUSP} = Mass of suspended sample

$$\text{Relative Density} = \left(\frac{\text{Apparent Specific Gravity}}{\text{Theoretical Density}} \right) \times 100 \quad (4)$$

Where:

Theoretical Density for SiC = 3.21 g/cm³

IV. RESULTS AND DISCUSSION

A. TGA Experiments

To highlight the characteristics of the weight loss curve, three values were used: 1) peak temperature, 2) intermediate temperature and 3) mass losses at the two characteristic temperatures. The characteristic temperatures are the intermediate and peak temperatures. The intermediate temperature (T_i) is the temperature that is associated with the peak of the first mass loss segment. The peak temperature (T_p) is the temperature at which the slope of the weight loss curve is smallest. The respective mass loss is that at both the peak and intermediate temperatures. An example of these can be seen in Figure 12 as the labeled points on the curves.

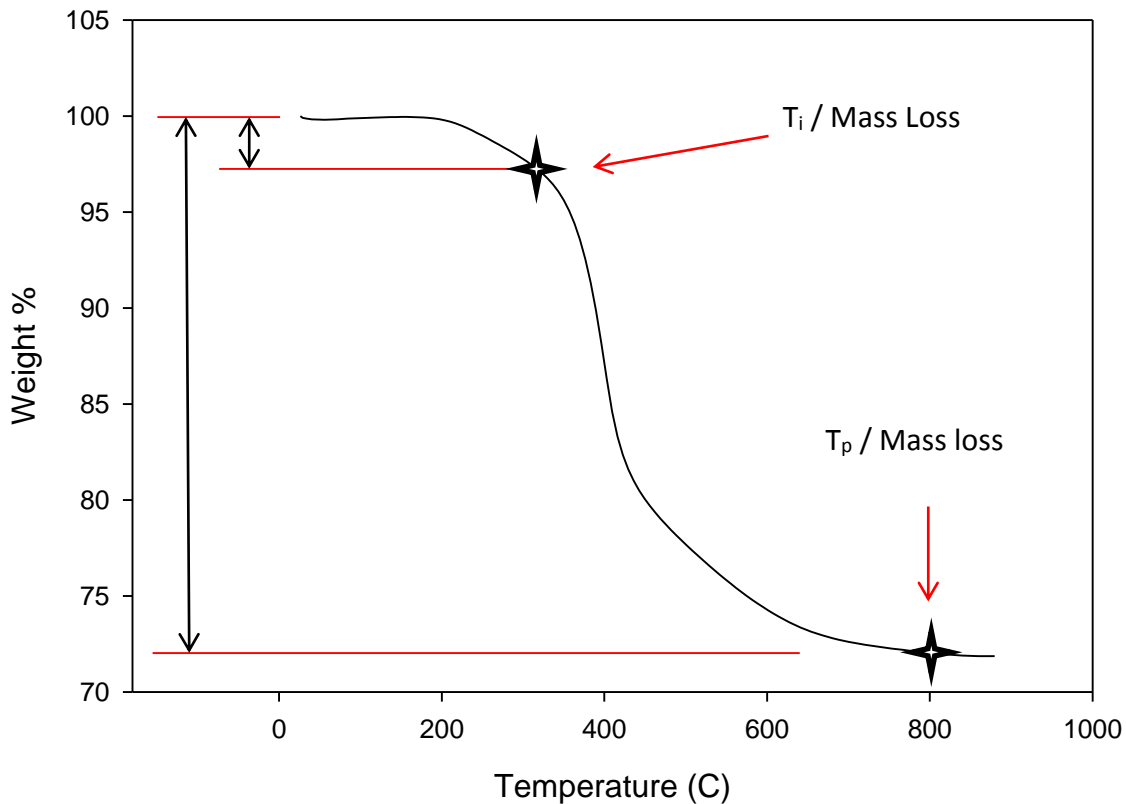


Figure 12. Schematic of TGA data

A.1 Standard Pyrolysis

This test was performed to understand the baseline pyrolysis performance for the SiC granules. From Figure 13, it is seen that the intermediate temperature is approximately 300°C and that there was consistent mass loss up to the peak temperature, suggesting that the weight loss was not complete (as compared to the weight loss in Figure 15). This pyrolysis cycle had a varying heating rate however, it was near 1K/min (see actual range in Section B of the Literature Review) along with a dwell at 400°C and 600°C for 120 minutes each.¹⁶ This method of pyrolysis retains 23.5 % wt. of expected carbon from the polymers (carbon data obtained by the true density method, not TGA). Although this yield is promising, the data shows that the weight loss is not complete. It is suggested that the peak temperature needs to be higher. The data in Figure 13 is normalized to the expected carbon yield. The expected carbon yield is the weight percent carbon in the cured phenolic structure, 78.5 wt. %. Therefore, to say that the data in Figure 13 resulted in a 23.5 % expected yield, it refers to a carbon yield of 18.4 wt. % of total phenolic resin (added).

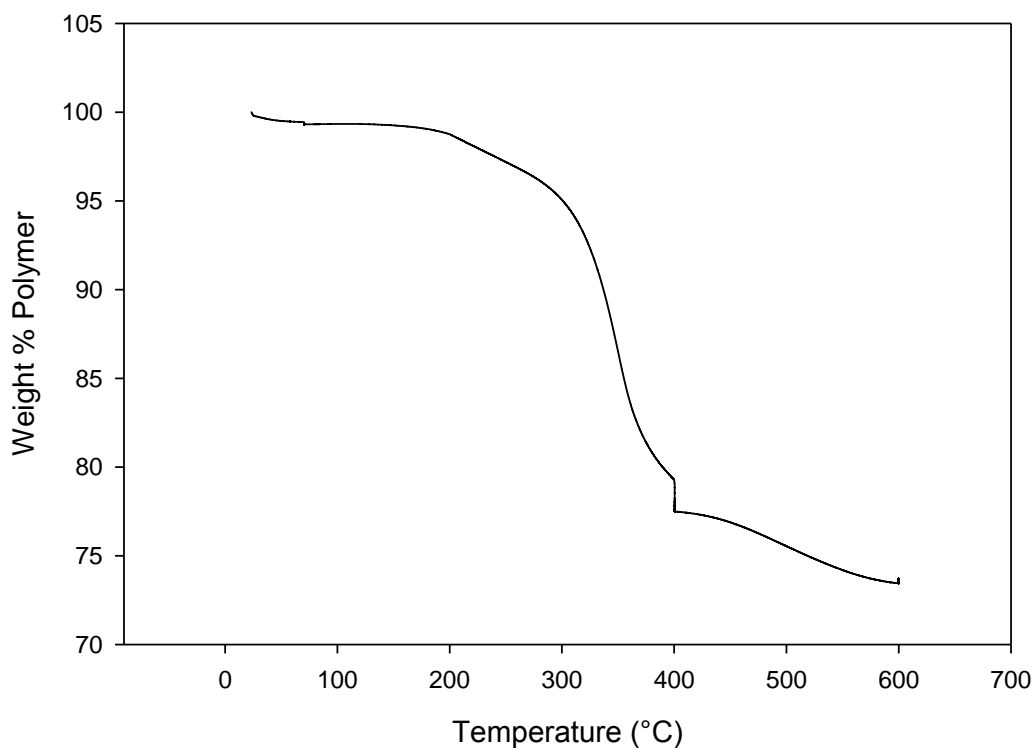


Figure 13. TGA of standard pyrolysis cycle

A.2 SiC Granules

SiC production granules were tested to map the baseline response to pyrolysis in air and nitrogen with varying heating rates. From these tests, heating rate and peak temperature were selected for the S.E.D. It is noted that these samples were all fired to 900°C with a gas flow rate of 100ml/min. Also, the gas chemistry was constant throughout the entire cycle (did not switch to another gas as in later experiments).

Figure 14 shows weight loss curves for the samples fired in air at different heating rates. All samples were pyrolyzed to a maximum temperature of 900°C. Both the peak and intermediate temperatures are lower than those pyrolyzed in a nitrogen atmosphere (Figure 15), suggesting a quicker reaction rate. Mass loss decreases with respect to heating rate and samples fired in air had a higher overall mass loss than those fired in nitrogen. Another observation is that high temperature oxidation was observed above 600°C when fired in air.

Figure 15 shows that when fired in nitrogen both peak and intermediate temperatures were high. Neither the intermediate nor peak mass loss showed a dependence on heating rate. Lastly, samples fired in nitrogen resulted in a higher yield than those in air.

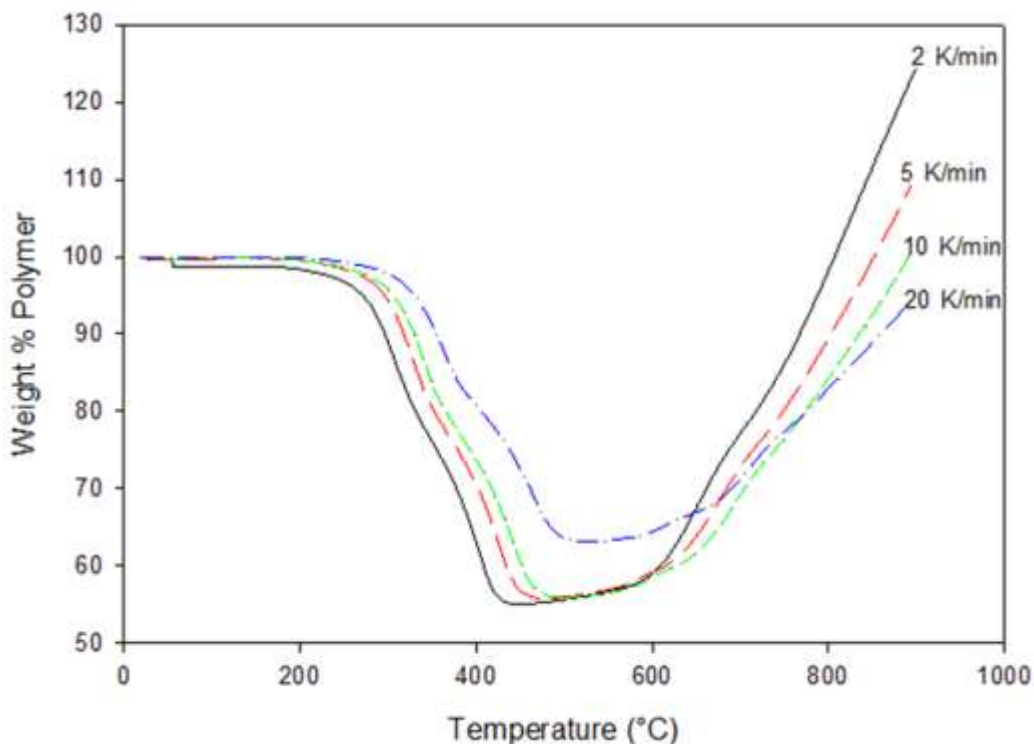


Figure 14. TGA of SiC granules in air

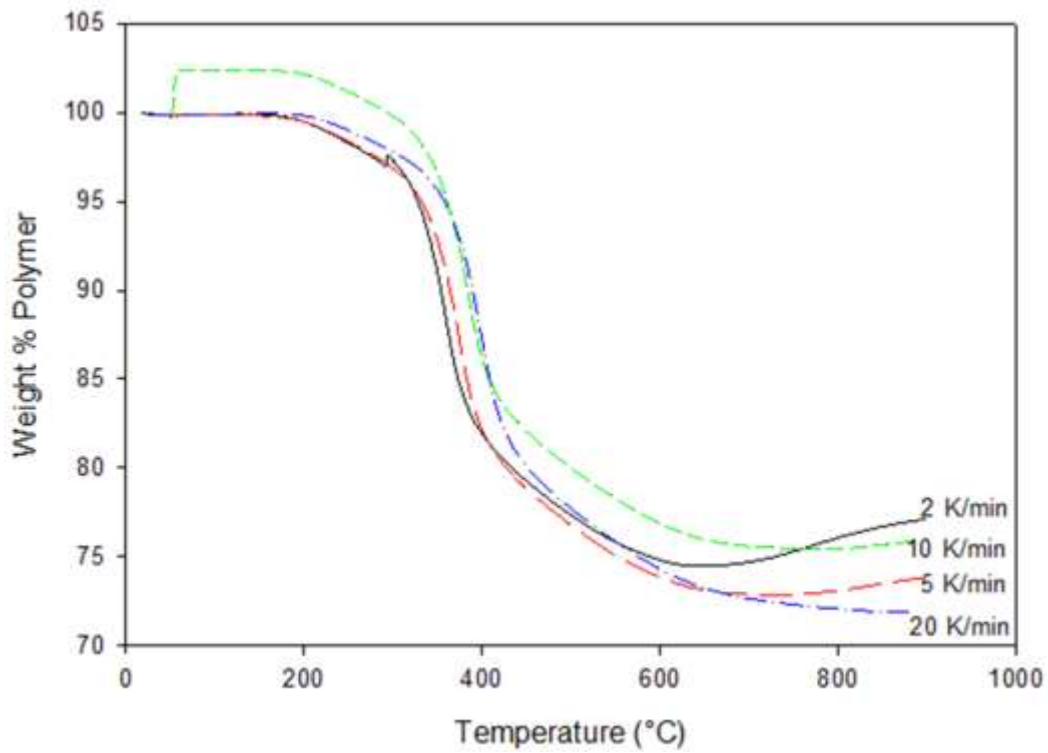


Figure 15. TGA of SiC granules in nitrogen

Figure 16 compares the results of the two atmospheres. Each plot is for the lowest tested heating rate, 2K/min. It shows a vast difference in mass loss when fired in air and nitrogen, nitrogen being favored for high yields. Figure 16 also shows that the characteristic temperatures are lowered in air.

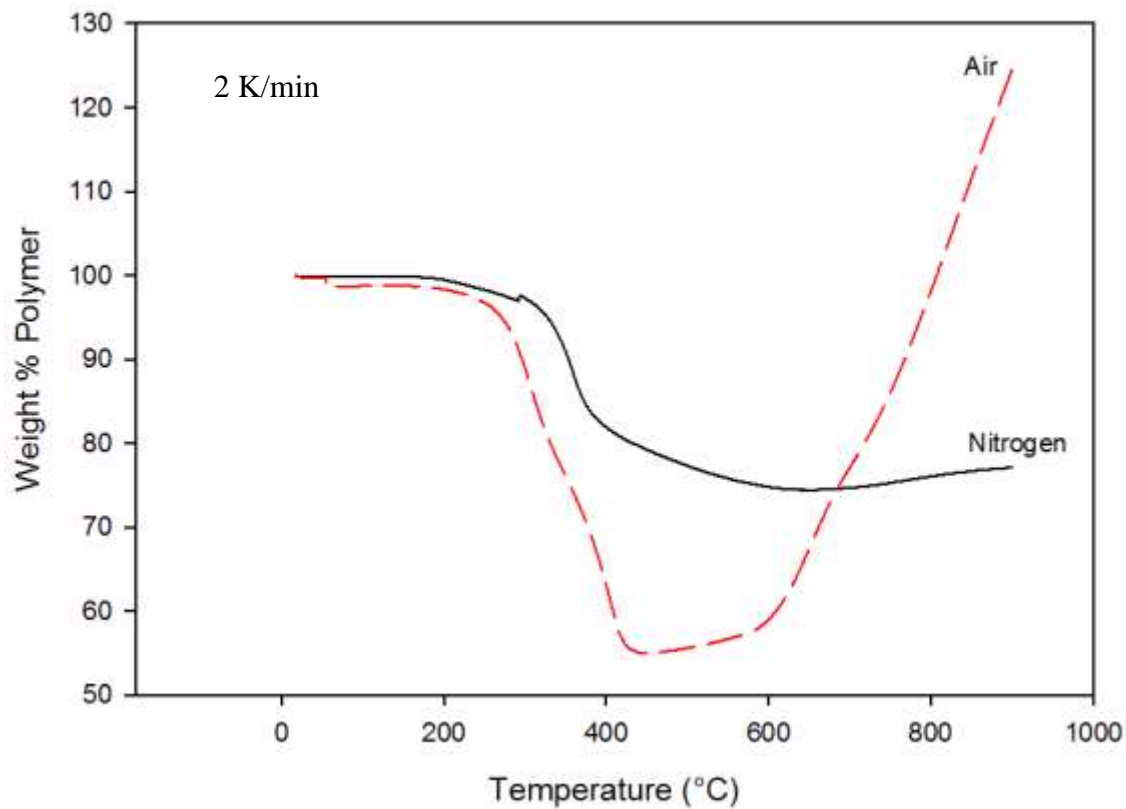


Figure 16. TGA of SiC granules in nitrogen and air

Figure 17 is a compilation of heating rate results. Samples in nitrogen exhibited higher characteristic temperatures than those in air and characteristic temperatures decrease as heating rate decreases for both atmospheres. Table VII shows the characteristic temperatures for the heating rate experiments in both nitrogen and air.

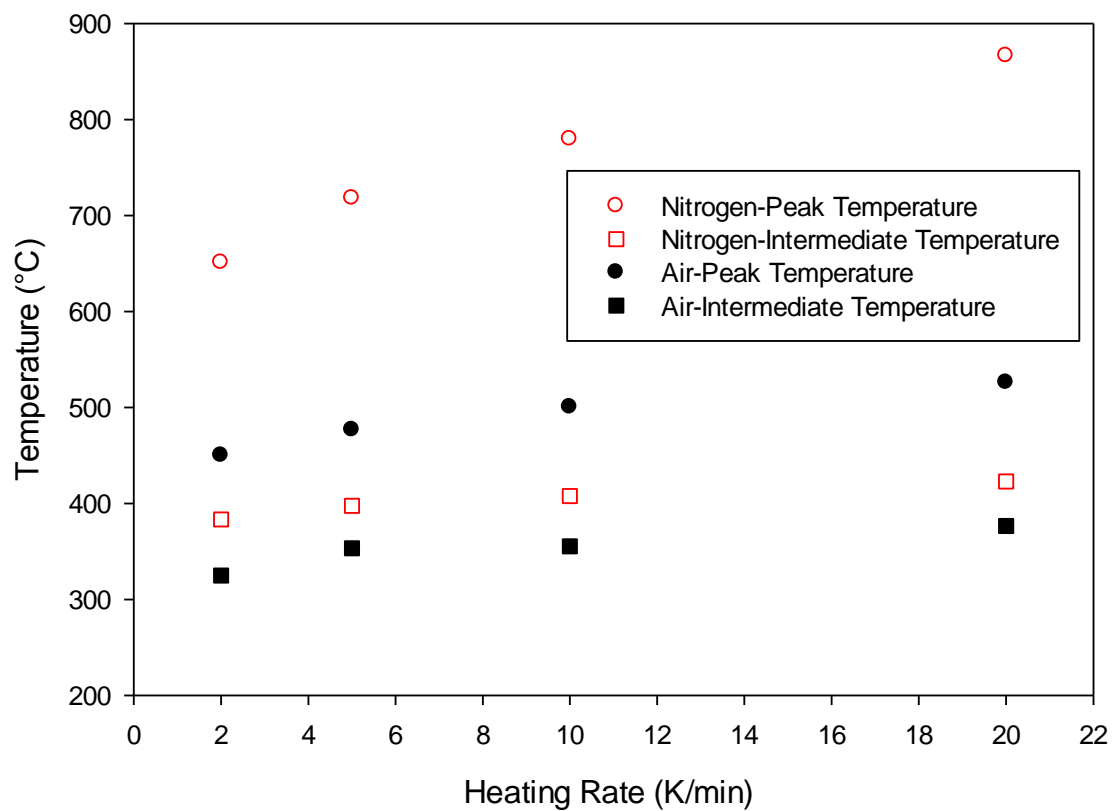


Figure 17. Extracted TGA data of SiC Granules. Characteristic temperature as a function of heating rate

Table VII. Characteristic temperatures for Pyrolysis in Nitrogen and Air

Heating Rate (K/min)	Intermediate Temperature (°C)		Peak Temperature (°C)	
	<i>Nitrogen</i>	<i>Air</i>	<i>Nitrogen</i>	<i>Air</i>
2	380	325	650	450
5	400	350	720	480
10	410	355	780	500
20	425	380	870	530

Figure 18 shows the relationship of peak temperature mass loss as a function of heating rate. This demonstrates that pyrolyzing in air results in higher weight losses regardless of heating rate. It also shows that the heating rate had a minimal effect on the mass loss amount if below 20 K/min.

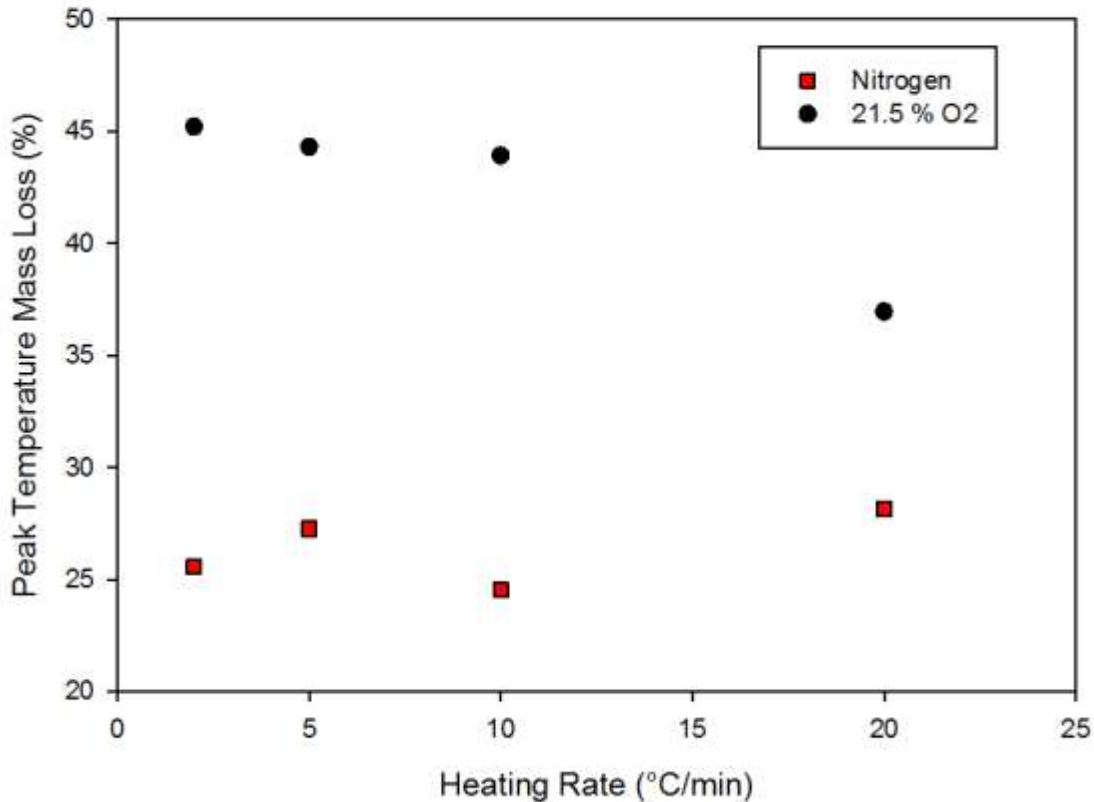


Figure 18. Extracted TGA data of SiC Granules: Peak temperature mass loss as a function of heating rate

The results showed the basic material behavior to heat treatment in different atmospheres. These tests showed that: 1) nitrogen yields lower mass loss, 2) nitrogen raises the characteristic temperatures, 3) a low heating rate results in low characteristic temperatures and 4) the average peak temperature in nitrogen was 750°C. The heating rate used in industry is near 1 K/min, the data supports this condition. A heating rate of 1K/min and a peak temperature of 750°C were chosen for the S.E.D.

A.3 Paraffin + Alumina Surrogate

These samples were conducted as a surrogate experiment to test if hydrogen stripping could change the pyrolysis yield of a simple linear hydrocarbon.

It was thought that a simpler polymeric structure (paraffin), would demonstrate the effects of hydrogen stripping more than a complex polymeric structure like cured phenolic resin. Paraffin consists of single-bonded carbons to form a chain backbone that is fully saturated with hydrogen. Because of the simple and predictable molecular structure of paraffin, the hydrogen level and loss (from pyrolysis) could be estimated.

Figure 19 is a plot of weight percent paraffin versus temperature when pyrolyzed in air. It is seen that there are dramatic weight losses associated with the dwell temperatures. Also, this plot shows that the peak weight loss both plateaus and varies with dwell temperature. The 200°C and 220°C dwells show that all the paraffin is lost at the peak temperature. Whereas, the lower dwell temperatures (150°C and 175°C) do have some residue remaining, approximately 20 wt.%. This shows that the mass loss is a function of the dwell temperature. The term “residue” is being used because it was not confirmed to be carbon by an elemental test, even though the material was heat treated to 900°C.

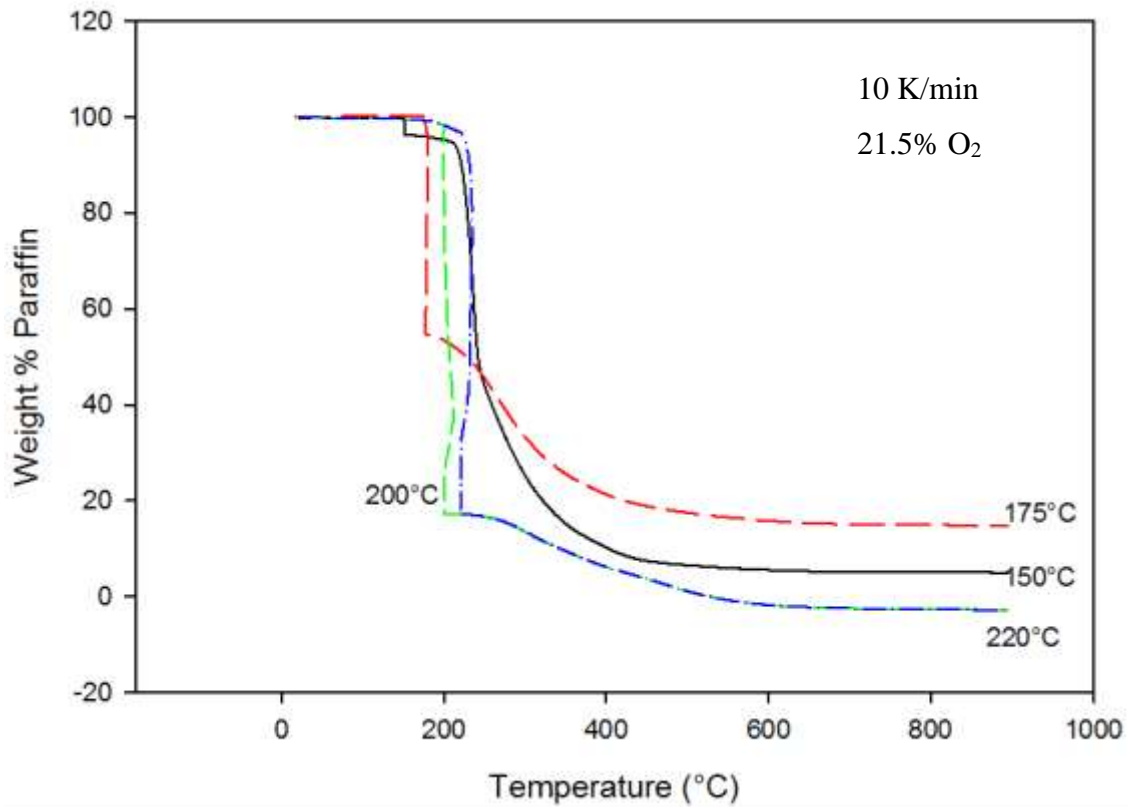


Figure 19. TGA of Paraffin + Alumina in 21.5% O₂

Figure 20 is a plot of weight percent paraffin versus temperature for samples fired in 5% O₂. This plot is similar to Figure 19 by how much weight is lost during the dwell however; almost every dwell temperature test resulted in no residue after the peak temperature. In 5% O₂, there are very little differences in the yields with changing dwell temperatures. This result shows a contribution of gas chemistry rather than dwell temperature for this atmosphere.

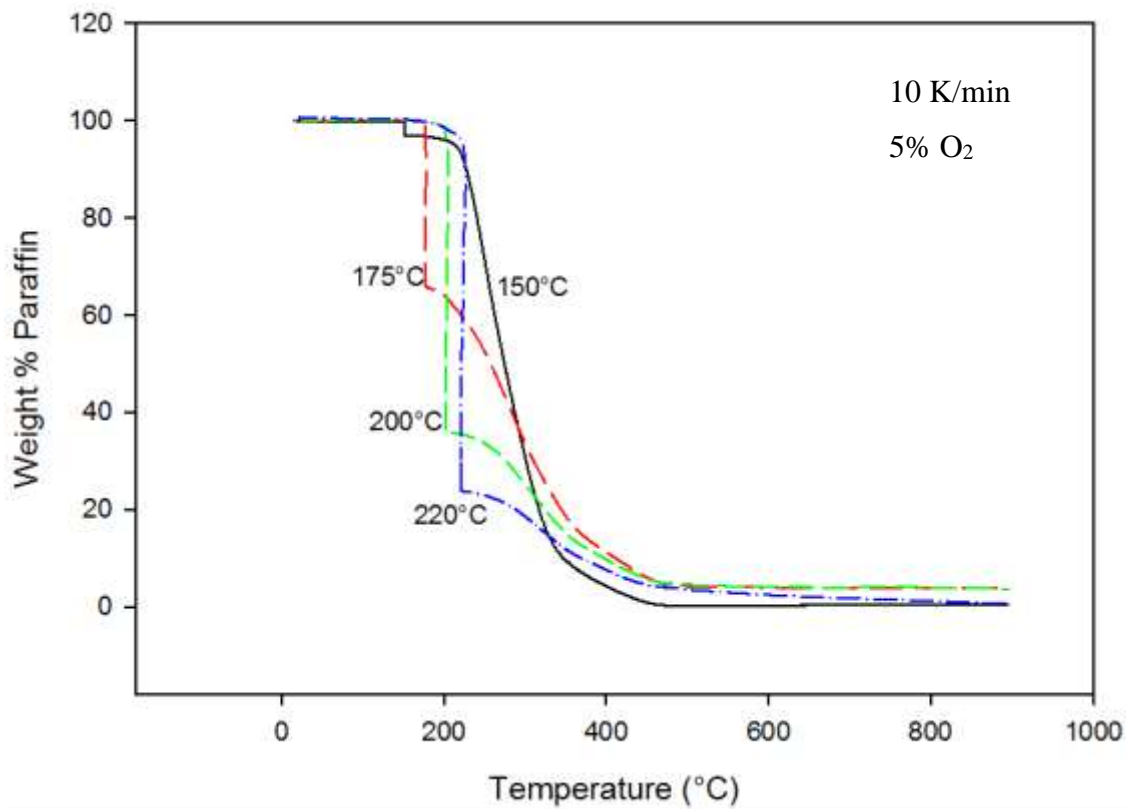


Figure 20. TGA of Paraffin + Alumina in 5% O₂

Figure 21 is a comparison plot of the TGA data for both 21.5% O₂ and 5% O₂, both tested at a dwell temperature of 175°C. This plot shows the difference the atmosphere had on the best performing dwell temperatures. It is seen that the yield from 21.5% O₂ (15 wt. %) was greater than the yield from 5% O₂ (4 wt. %).

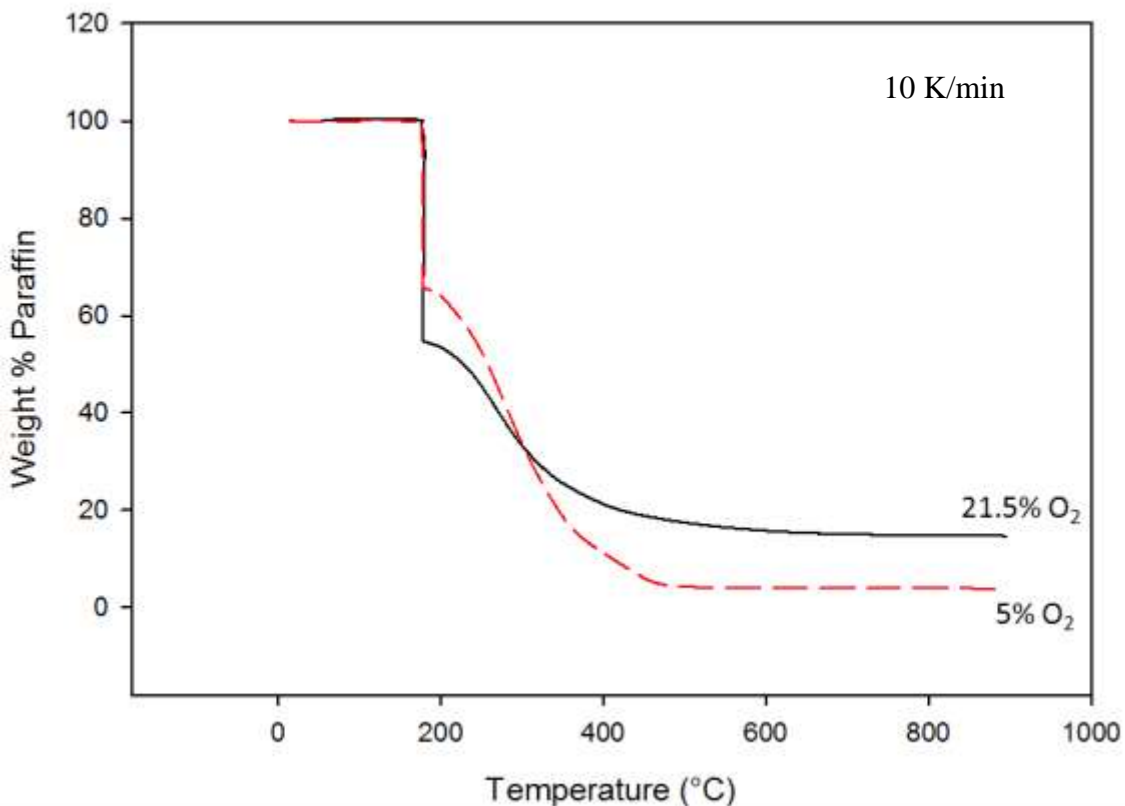


Figure 21. TGA of Paraffin + Alumina air and 5% O₂ comparison, 175°C dwell

To depict the performance of the hydrogen stripping hypothesis, residue data was calculated and plotted for both after the dwell temperature and after the peak temperature. The stoichiometry of the paraffin was assumed based off of the melting temperature. It was found that the main constituents were C₂₅H₅₂ and C₃₀H₆₂.²⁶ Since the chemistry is known, the weight percent's of each, C and H, can be calculated. It was found that if hydrogen and oxygen were stripped from the structure, 85.3 wt% of the material would be left (in the form of C). The 85.3% yield was considered the “expected” residue. Figure 22 shows this on a plot of maximum carbon yield versus moles of carbon in the paraffin. The high and low refer to the stoichiometries of paraffin that best describe the melting temperature of the material used (high and low moles of carbon). The dashed line is the average of the two compounds.

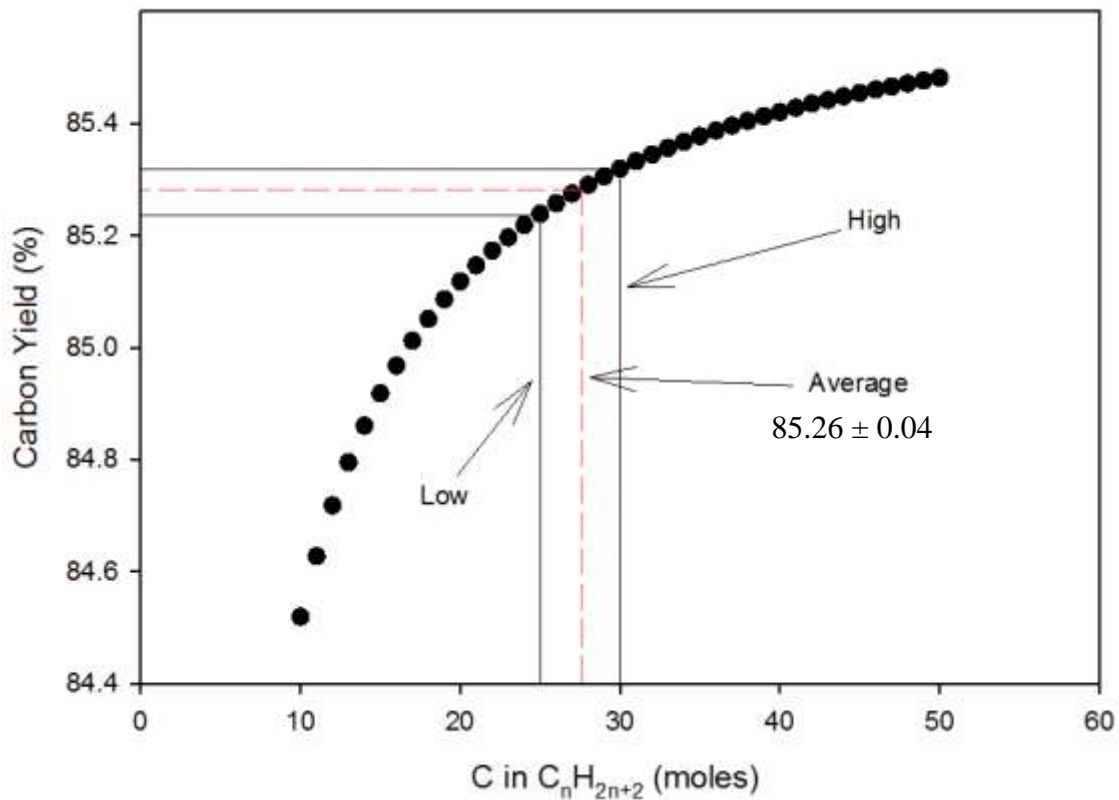


Figure 22. Maximum carbon yield as a function of paraffin stoichiometry

Figure 23 is a plot of the residue after the dwell temperature (% expected) versus dwell temperature. It shows how the weight loss is affected by both the dwell temperature and the gas chemistry. It is seen that the highest residue is obtained with both a low dwell temperature and either oxygen level (5% O₂ is favored as dwell temperature increases). For the data corresponding to a dwell at 150°C, the residue is larger than 100% expected because the weight that was lost did not amount to the weight of hydrogen in the sample. The data was selected around the point where the mass loss ends (during the dwell), as to obtain an average and standard deviation. The error is so small the bars are within the data points. It is important to understand that although these results look promising, the pyrolysis is not yet complete. After these temperatures, the gas was switched to nitrogen and brought to 900°C.

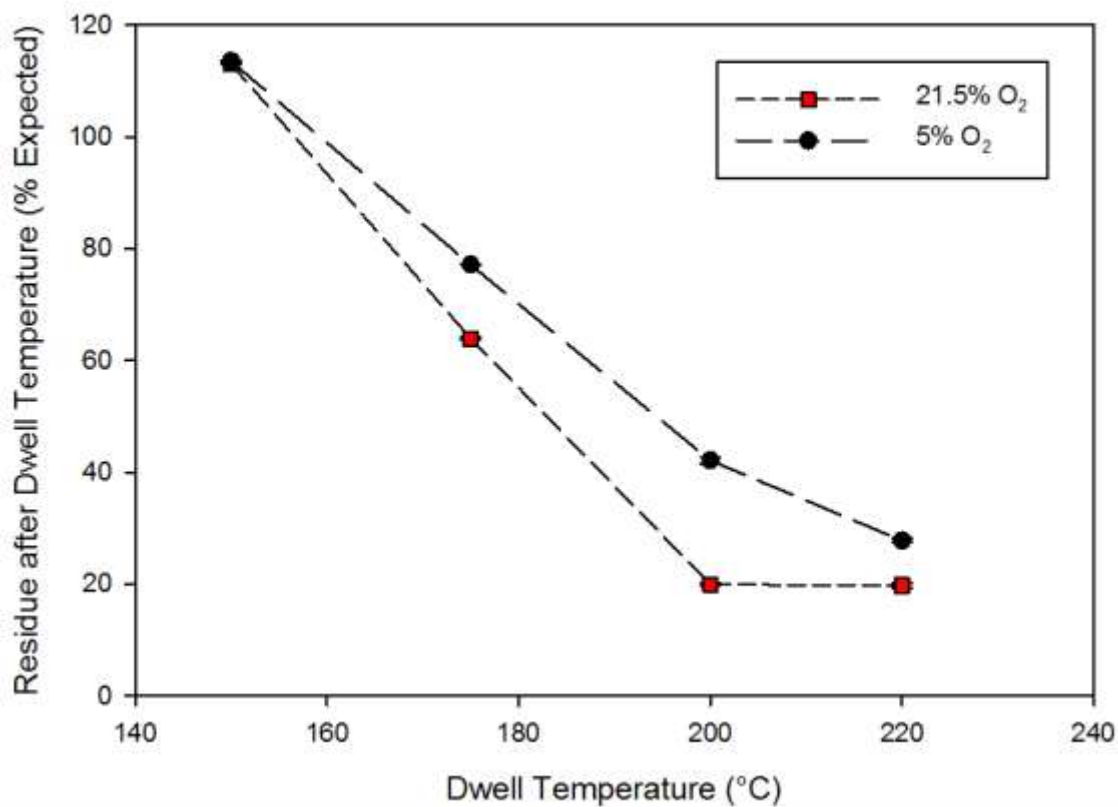


Figure 23. Extracted TGA data of Paraffin + Alumina. Plot of % expected residue after the dwell temperature as a function of dwell temperature

Figure 24 shows the residue after the peak temperature was reached. It is a plot of residue as a percent of the expected versus dwell temperature. There seems to be no true correlation between final residue, dwell temperature or oxygen level. 175°C seems to be a transition point; residue is high below a 175°C dwell, if air is used. If the dwell temperature is increased, lower oxygen content seems favorable. The data was sampled at the beginning and end of the mass loss event around the peak temperature. The complete removal of the paraffin in the samples pyrolyzed in 5% O₂ above a 175°C dwell temperature showed that paraffin is not a good surrogate for phenolic resin. It was found that linear hydrocarbon chains tend to fully depolymerize via chain scission, resulting in little to no residual carbon.²⁷

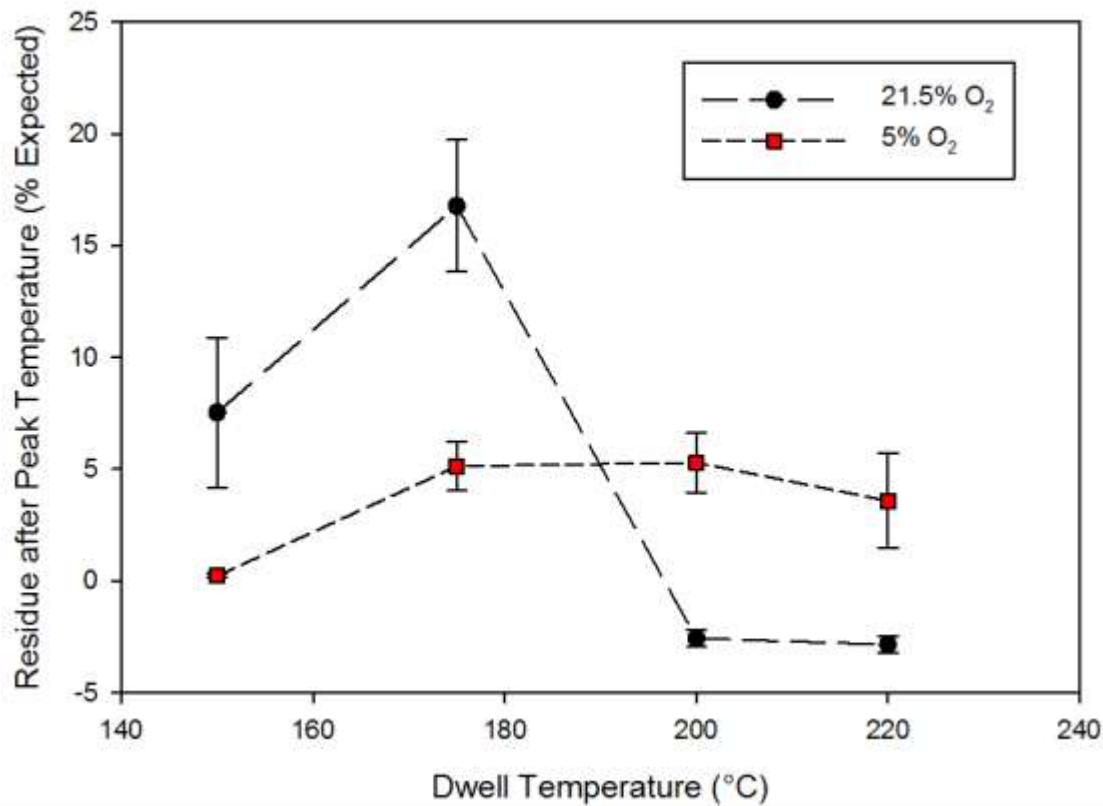


Figure 24. Extracted TGA data of Paraffin + Alumina

The results show that a preferred weight loss event is present after the dwell temperature which displayed promising results however, when fully heat treated, these effects were diminished. What was learned from these tests is that yield can be increased if a low dwell temperature and increased oxygen levels are used. This result helps validate the hypothesis that hydrogen stripping during pyrolysis can increase carbon yields.

The data also exhibits promising results for those processes that have the goal of a clean burnout. If the burnout process has a low dwell temperature, a slightly oxidative environment is suggested. If a high dwell temperature is used, burning out in air is more successful.

A.4 Phenolic + Alumina Pyrolysis

Experiments with phenolic resin and alumina were used to determine the pyrolysis characteristics of the resin without the other polymeric processing aids. A series of experiments

with atmosphere and dwell temperature as variables were conducted. All of the plots for phenolic and alumina have been normalized to the amount of phenolic added.

Figure 25 shows the weight change TGA data for phenolic and alumina samples fired in 2% O₂. The different series refer to the different dwell temperatures. It can be seen that the lowest dwell temperature gave the lowest weight loss. Figure 26 is a plot of weight percent phenolic versus dwell time in 2% O₂. This plot highlights weight losses during the 60 minute dwells for the different dwell temperatures. It is seen that a dramatic increase in weight loss during the dwell happens with increased dwell temperature. The 200°C dwell temperature showed the best yield.

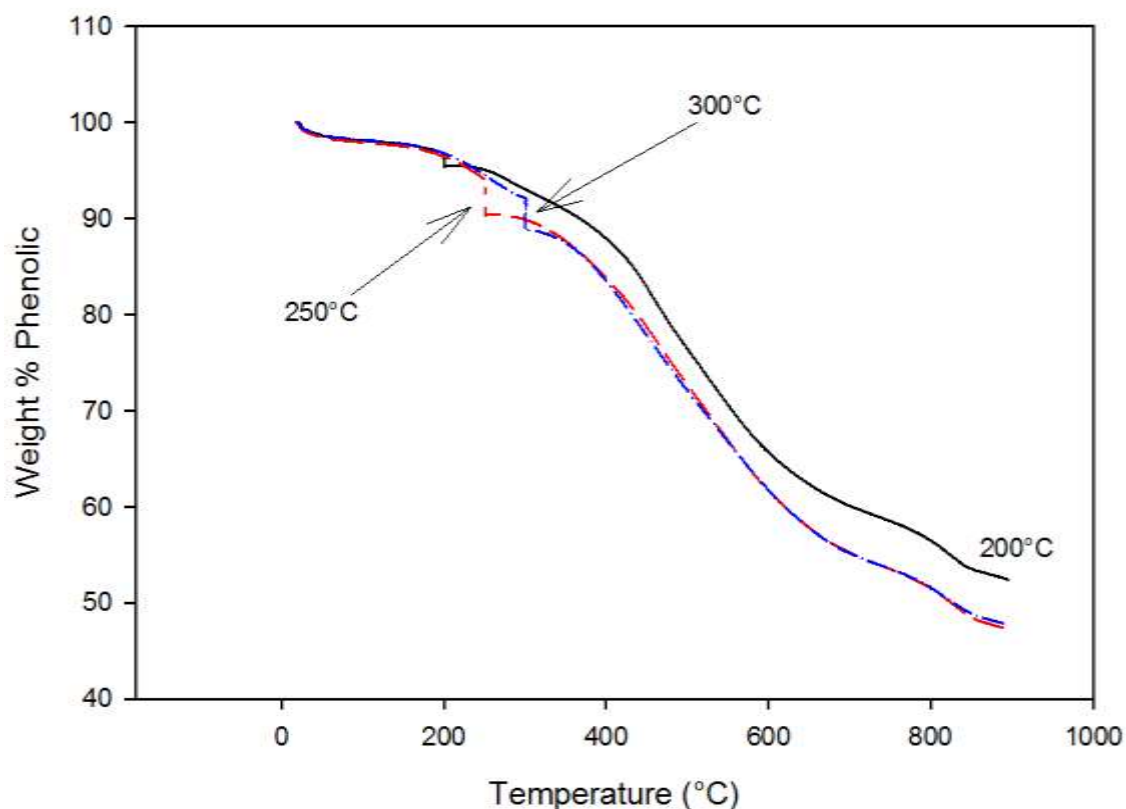


Figure 25. TGA of Phenolic + Alumina in 2% O₂

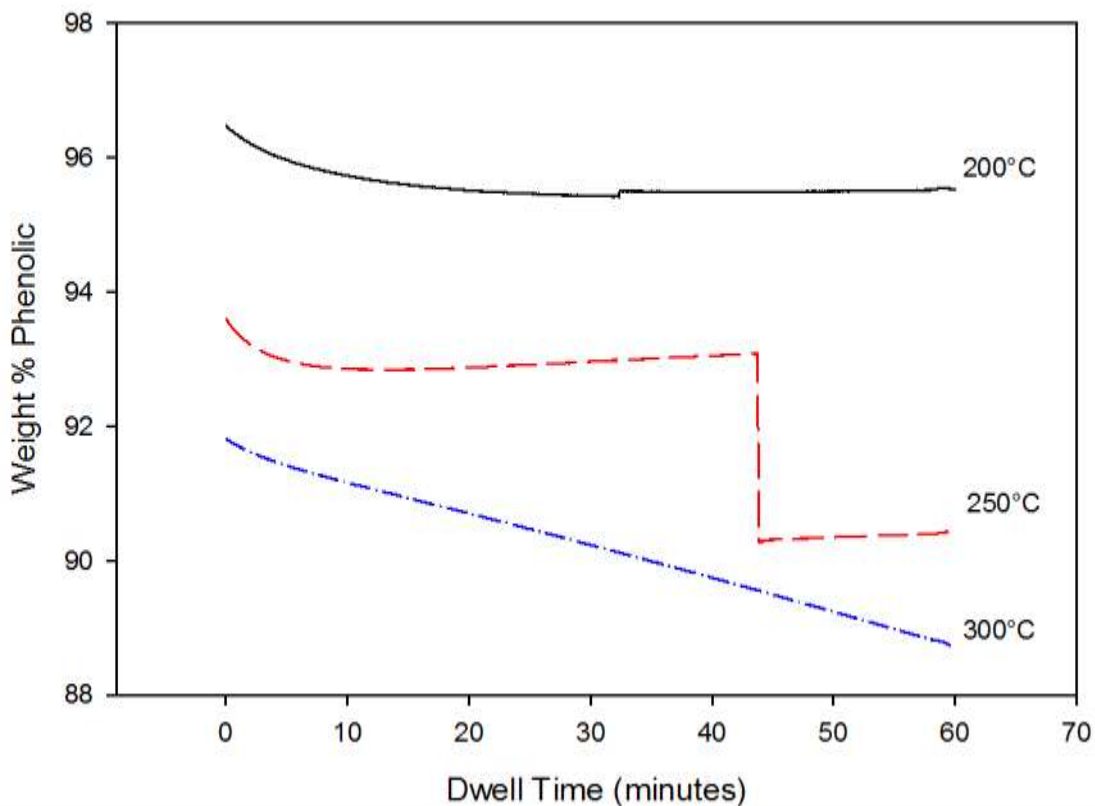


Figure 26. Weight loss during the dwell period, in 2% O₂

Figure 27 shows the weight change TGA data for phenolic and alumina samples fired in 5% O₂. The different series refer to the different dwell temperatures. Again, the lowest dwell temperature gave the highest yields. The yield from the 200°C dwell is slightly higher than when pyrolyzed in 2% O₂. Figure 28 is weight percent phenolic versus dwell time in 5% O₂. Again, it is seen that the higher dwell temperature promotes an increase in mass loss throughout the dwell period. It shows that the 200°C dwell temperature starts to lose a minimal amount of mass and then starts to gain mass near the end of the dwell.

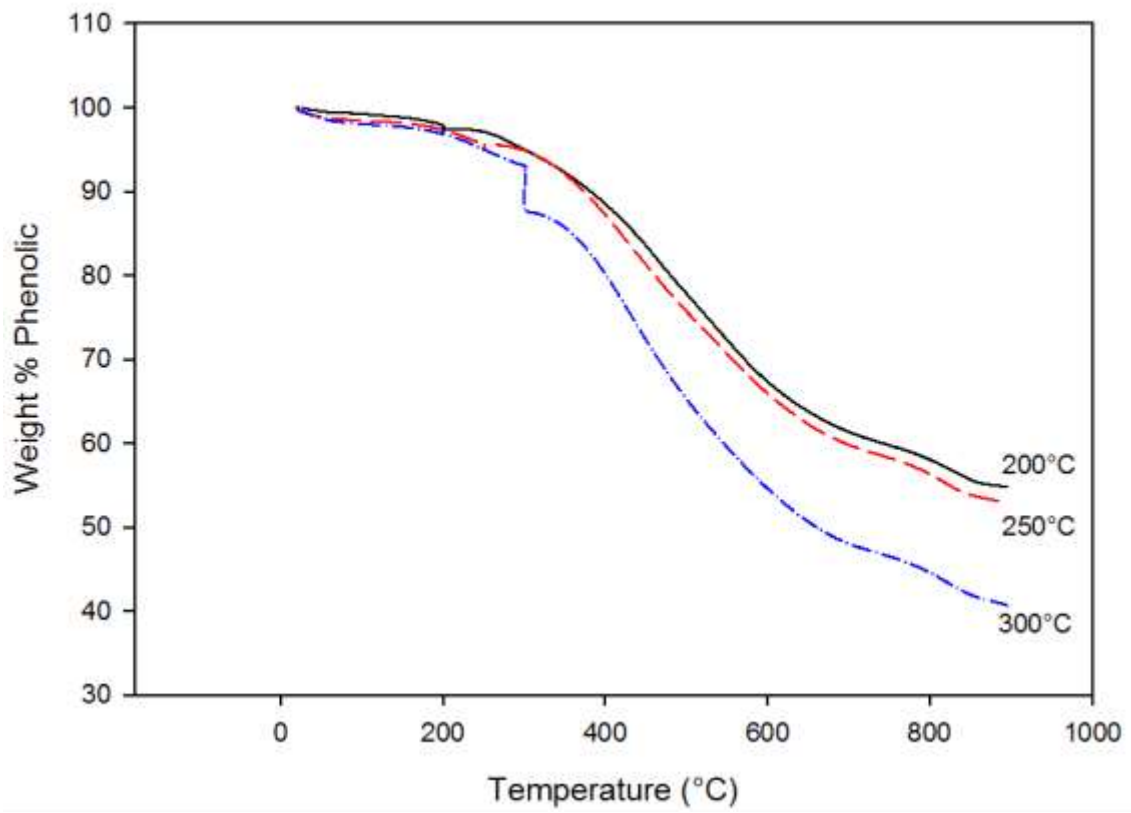


Figure 27. TGA of Phenolic + Alumina in 5% O₂

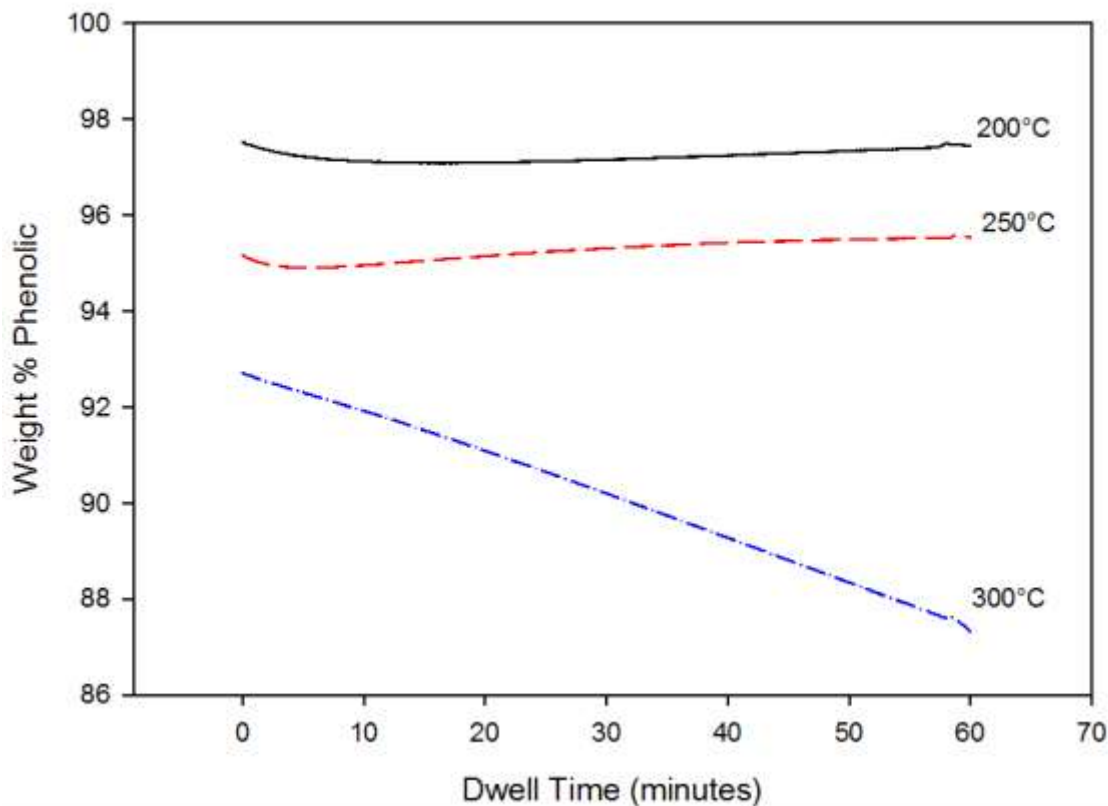


Figure 28. Weight loss during the dwell period, in 5% O₂

Figure 29 shows the weight change TGA data for phenolic and alumina samples pyrolyzed in 21.5% O₂. The different series refer to the different dwell temperatures. Again, the lowest dwell temperature gave the lowest weight loss. This experiment shows a larger difference in the final weight loss as a function of dwell temperature than the previous experiments. Also, firing in 21.5% O₂ resulted in a higher weight loss than the experiments with a lower oxygen level. Figure 30 is a plot of the weight loss as a function of dwell time for pyrolysis in air. Mass gain is seen in the dwell period for the 200°C case. This can be seen in the 200°C curve in Figure 29 as the vertical increase at 200°C. There is a tendency for this behavior to be “written-off” as an instrumental error however, Figure 30 shows that this is not instrumental error and that there is a consistent mass gain event during the dwell for this temperature and atmosphere.

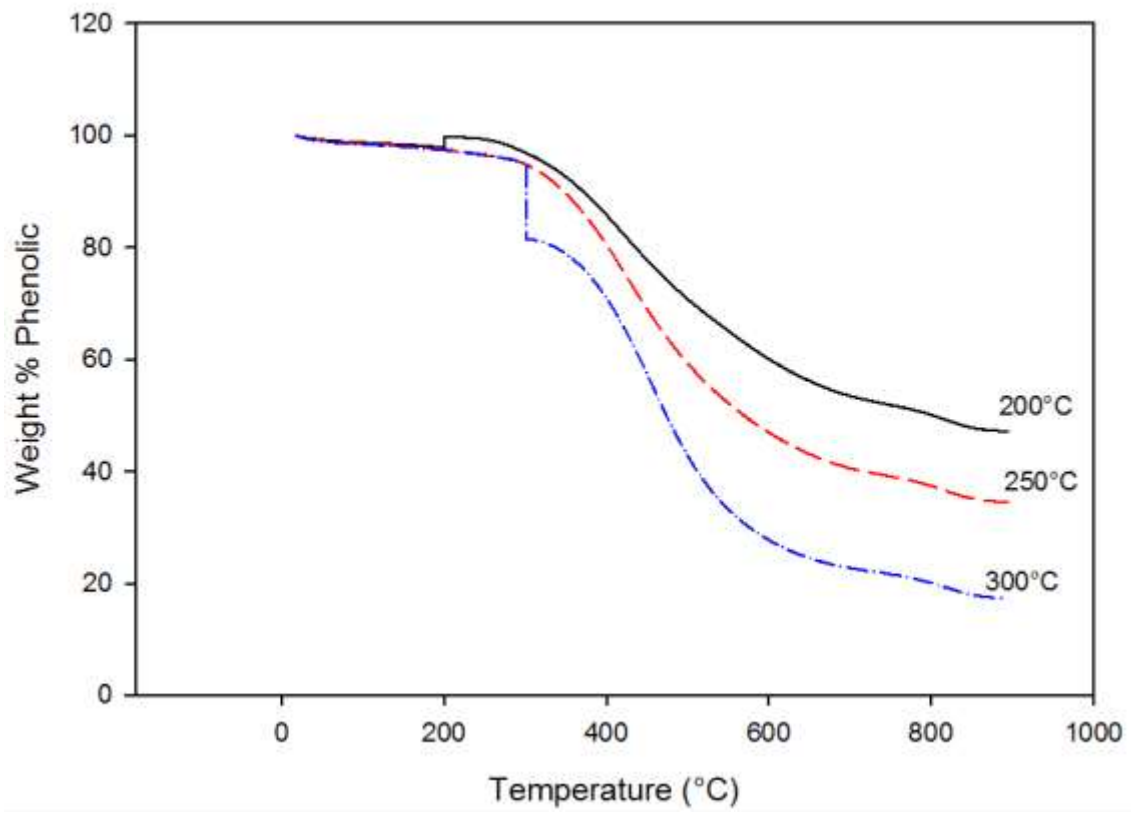


Figure 29. TGA of Phenolic + Alumina in air

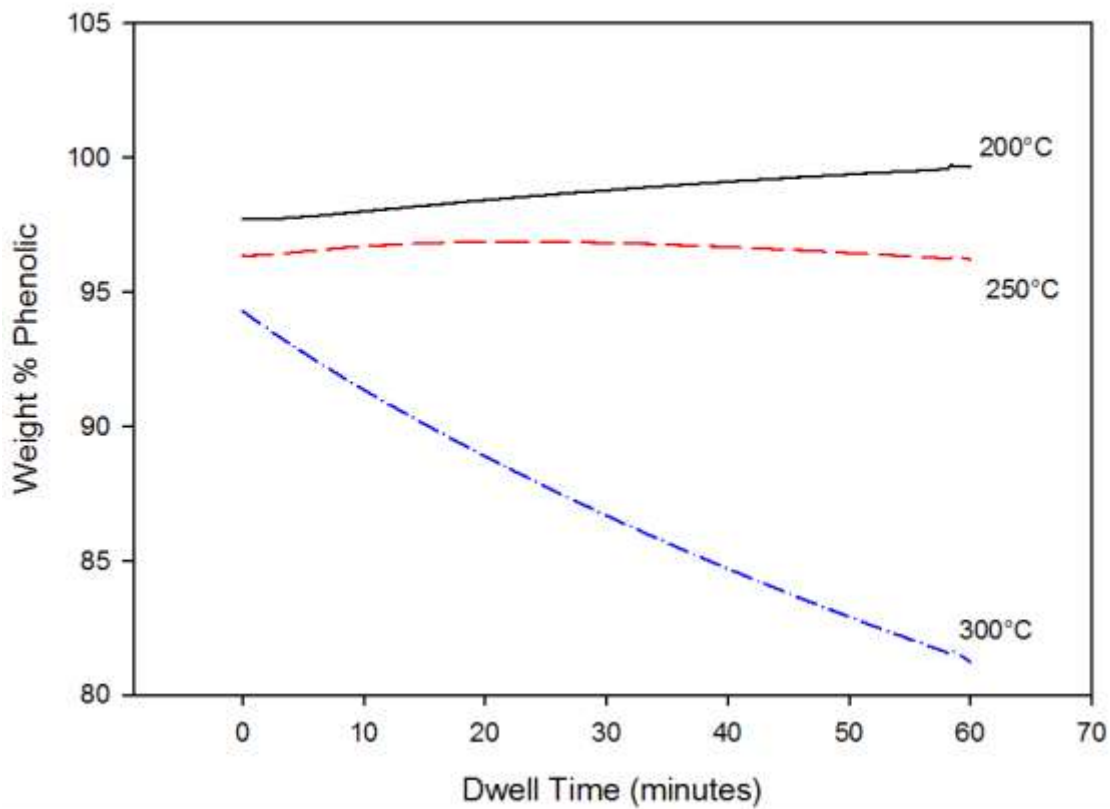


Figure 30. Weight loss during the dwell period, in air

Figure 31 is a comparison plot of phenolic and alumina TGA data. The plot represents the 200°C dwell curve for each atmosphere, the best performing dwell temperature. It shows that the atmospheres with less O₂ have a higher yield than in air. This is the opposite than what was observed in the paraffin tests. Figure 32 is the plot of weight loss during the dwell period. This plot compares the dwell period weight loss of the different atmospheres all pyrolyzed with a 200°C dwell. Although the pyrolysis in air shows promising mass loss results in Figure 32, when the entire range of pyrolysis is examined (Figure 31) it is seen that it does not perform best.

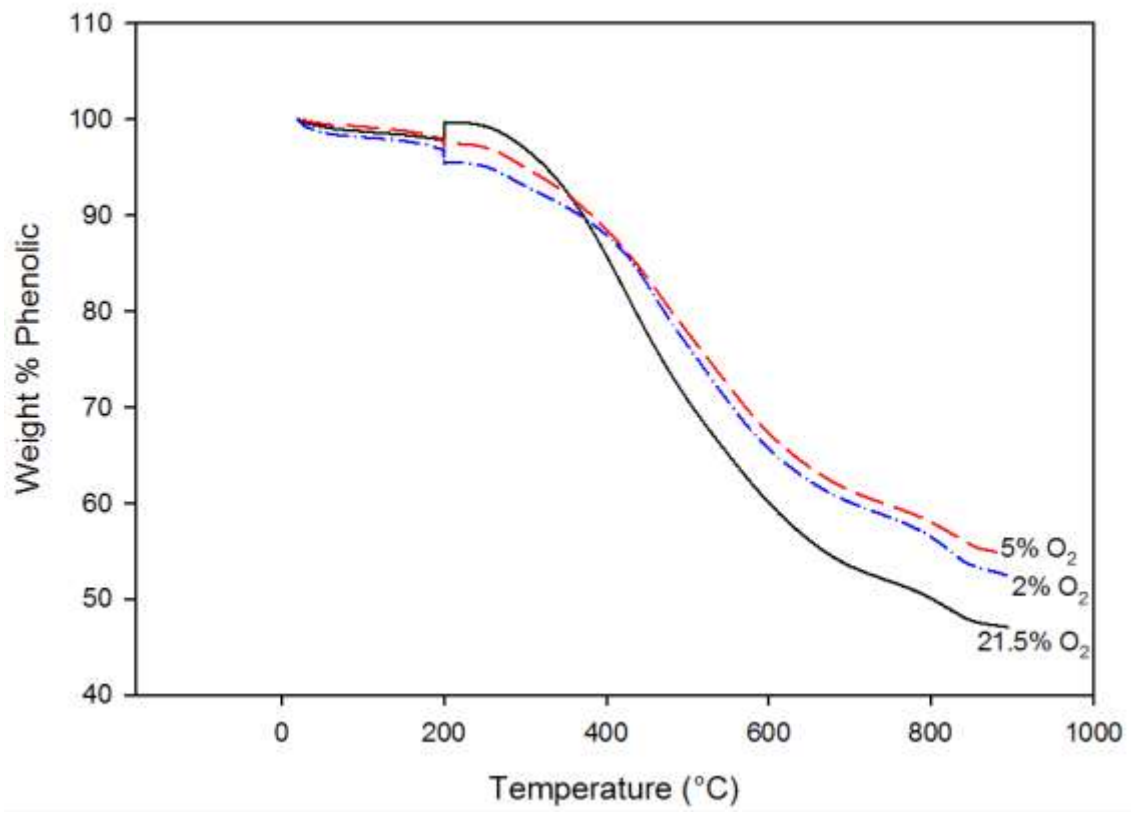


Figure 31. TGA of Phenolic + Alumina comparison, 200°C dwell

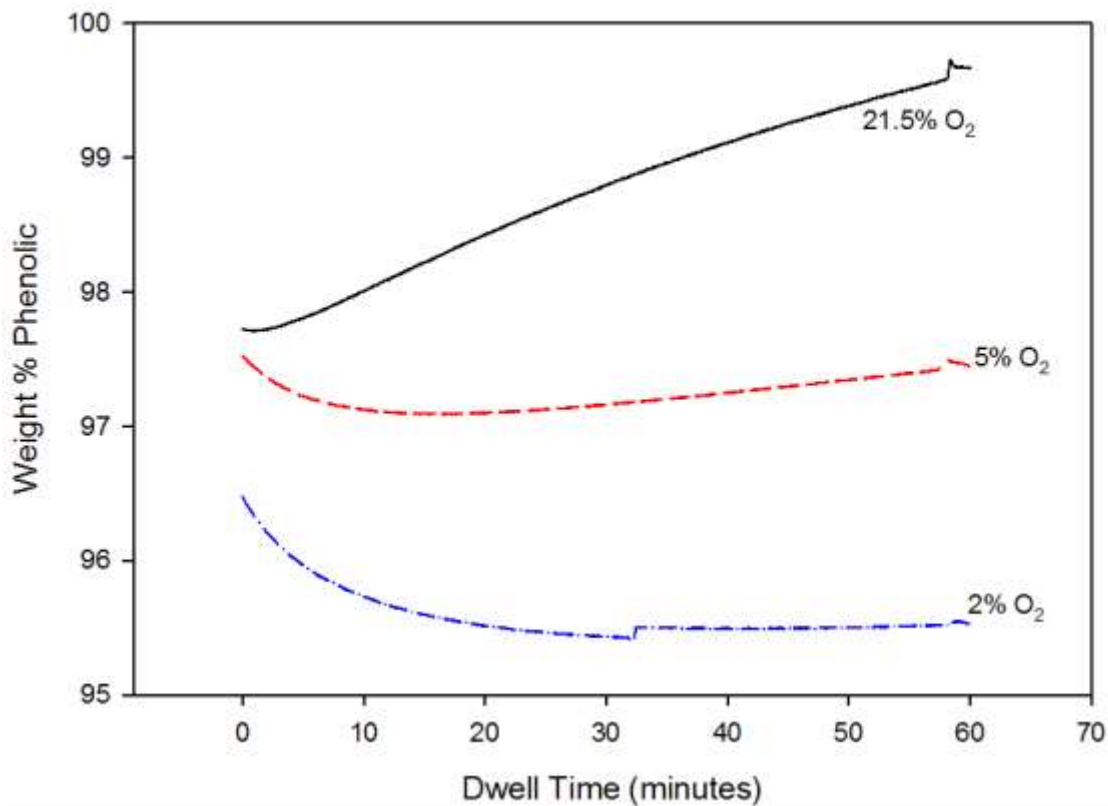


Figure 32. Weight loss during the dwell period, 200°C dwell temperature

Using the proposed cured, phenolic structure (Figure 7), a theoretical molecular weight can be calculated. This also allows the weight percent of hydrogen and oxygen to be calculated. Therefore, a theoretical “expected residue” can be calculated (simply the mass fraction of carbon in the mer). This expected residue is the maximum amount of carbon that can be obtained from pyrolysis. This maximum carbon yield is 78.5 wt% of total (dried) phenolic resin.

Figure 33 and 34 plots the residue as a function of dwell temperature for both residues post dwell and residue post peak temperature. These plots have been normalized to the “expected residue” meaning that the axis is the percentage obtained of the theoretical maximum carbon yield. The error bars in these figures are smaller than the symbols. Figure 33 is a plot of percent residue after dwell as a function of dwell temperature. Two correlations can be seen in this plot: 1) lower dwell temperatures results in higher residue and 2) 21.5% O₂ resulted in the highest residue at a low dwell. The data is above 100% because it is plotted as % expected. The

residual that is present after the dwell is an artifact of not removing all of the hydrogen present therefore, showing yields above 100%. This data will not characterize how the material pyrolyzed overall however it is used to understand how the different atmospheres and dwell temperatures change the results half way through pyrolysis.

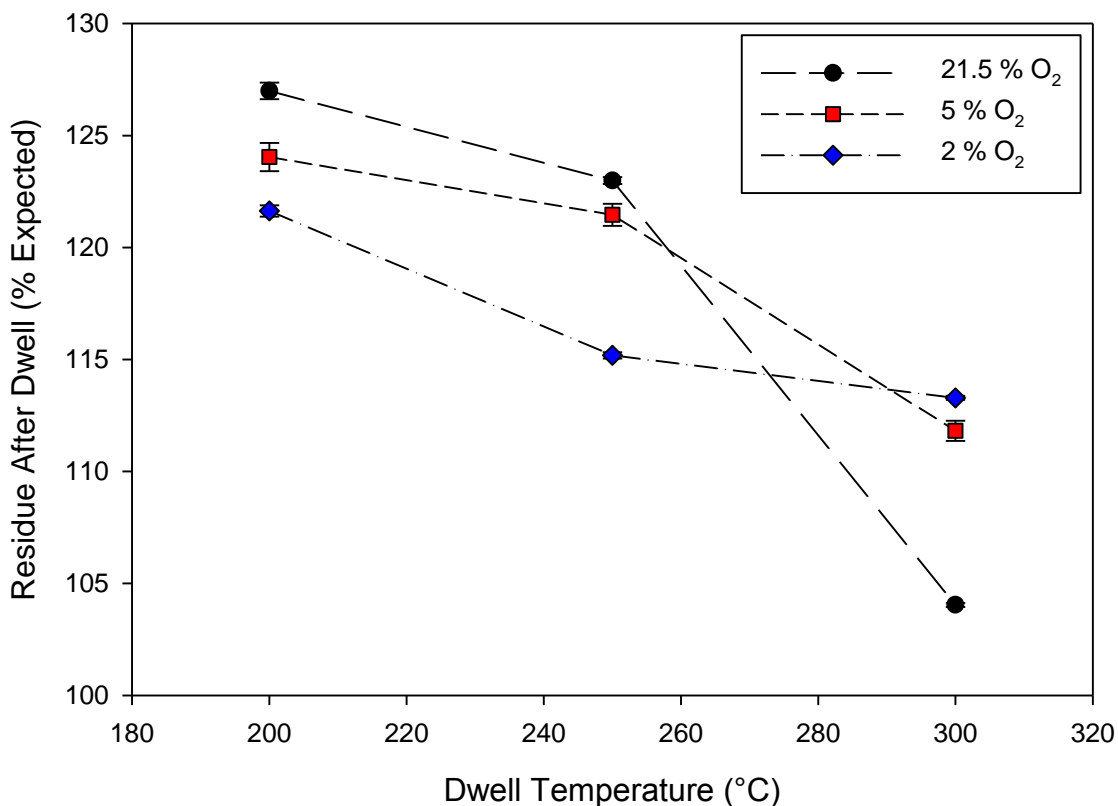


Figure 33. TGA Residue data of Phenolic + Alumina, residue after dwell

Figure 34 is a plot of percent residue after the peak temperature versus dwell temperature. This is showing the overall yields from pyrolysis as a function of dwell temperature. Again, a low dwell temperature gives the highest yield. Now, the lower O₂ levels are performing better than 21.5% O₂. At a dwell temperature of 200°C, 5% O₂ gives the best yield of about 78% expected.

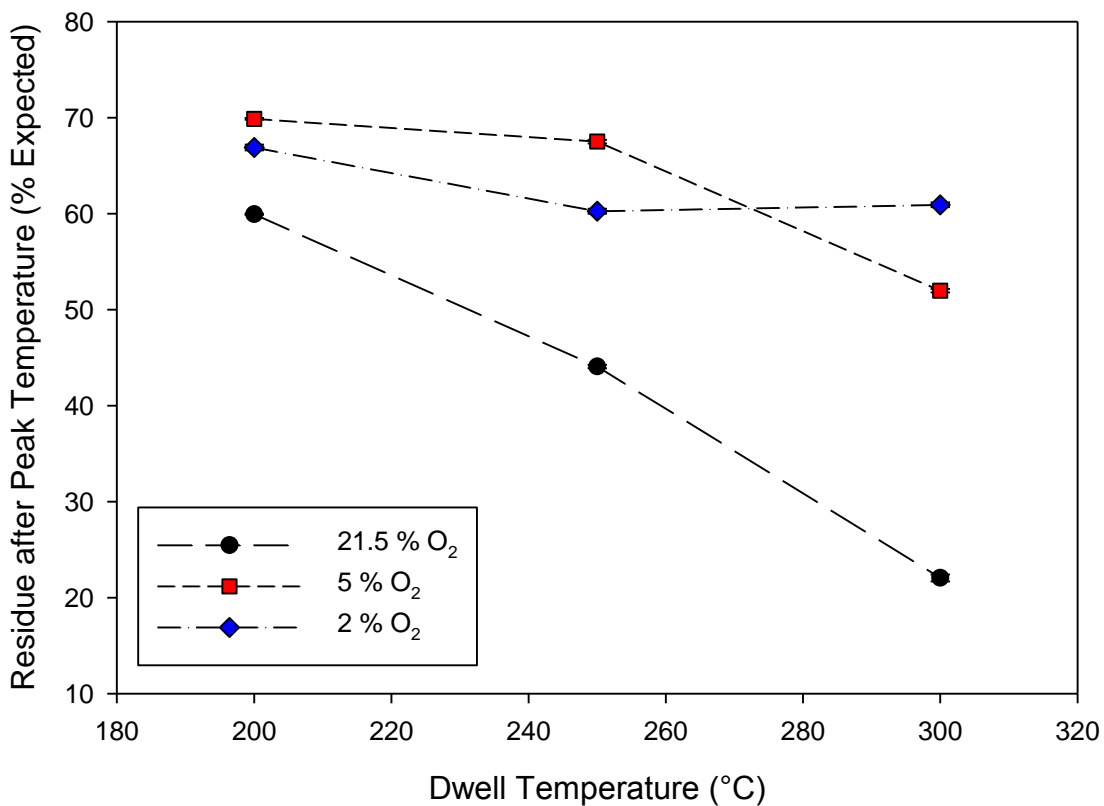


Figure 34. TGA Residue data of Phenolic + Alumina, residue after peak temperature

Two things were learned from these tests first, low dwell temperatures are important in maximizing the yield from phenolic resin and second, there is a contribution from the oxygen level. It has been established that pyrolyzing in air does not yield the best results however; having 2% or 5% O₂ resulted in high expected residue rates. These experiments gave a better understanding of how this material reacts to different environments and temperatures during pyrolysis.

B. S.E.D. Experiments

A statistical experimental matrix was created to test the variables, and their corresponding levels. Information obtained from industry, literature and TGA experiments helped to narrow variables and their levels to be tested. TGA showed that oxygen level and dwell temperature were important to pyrolysis while the importance of flow rate was observed by industry.

The responses to the experimental design evolved during analysis and include weight loss, sintered density, LECO carbon analysis, carbon content via bulk density and microstructural analysis. Microstructural analysis was a supplemental response, intended to visually depict changes in microstructure and was not included in the S.E.D. All responses were individually analyzed in Design Expert, which performs model fit calculations and reduces the chosen models to better represent the data. Table VII shows the labels given to each factor when describing the ANOVA results and the experimental results.

Table VII. S.E.D. Factor Labels and Names

Factor Label	Factor Name
A	Flow Rate
B	Atmosphere
C	Dwell Temperature

The ANOVA results outputs a sum of squares value, df, mean square, F value and a p value. The sum of squares is the sum of squared deviations from the mean. The term df refers to the degrees of freedom for the term. Mean square is the variance associated with the term. The F value is a test that compares the variance of the term with the residual variance; a large F value is desired for significance. The p value is the probability value associated with the F value; it measures the statistical significance of the variable. It states the probability of getting an F value if the term did not have an effect on the response. If the p value is less than 0.05 the term is significant, if it is larger than 0.1 the term is not significant. All responses in the S.E.D. showed normality in the data, no effect of run order or residuals and did not need transformation. A table of the S.E.D. runs, parameters and response data is in Section A of the Appendix.

B.1 Response: Sintered (Relative) Density

Samples were intentionally undersintered to exaggerate any differences in the microstructure that pyrolysis may cause. With an industry identified sintering temperature of 2165°C, samples were fired to 2100°C, 2050°C and 2000°C. Although the objective was to undersinter, high densities are desirable.

The first sintering run was to 2100°C and resulted in high densities, 97%. Due to the high density at 2100°C, samples were then sintered at 2050°C and 2000°C. Relative density was measured via the immersion technique.²⁵ Figure 35 shows relative density and apparent porosity versus sintering temperature for all the S.E.D. sintering data. It can be seen that there is a diminishing effect of increasing sintering temperature with density showing good densification. The same effect can be seen with porosity. None of the sample sets showed statistically significant differences in density. The data in this plot is all of the density and porosity data obtained from the S.E.D.

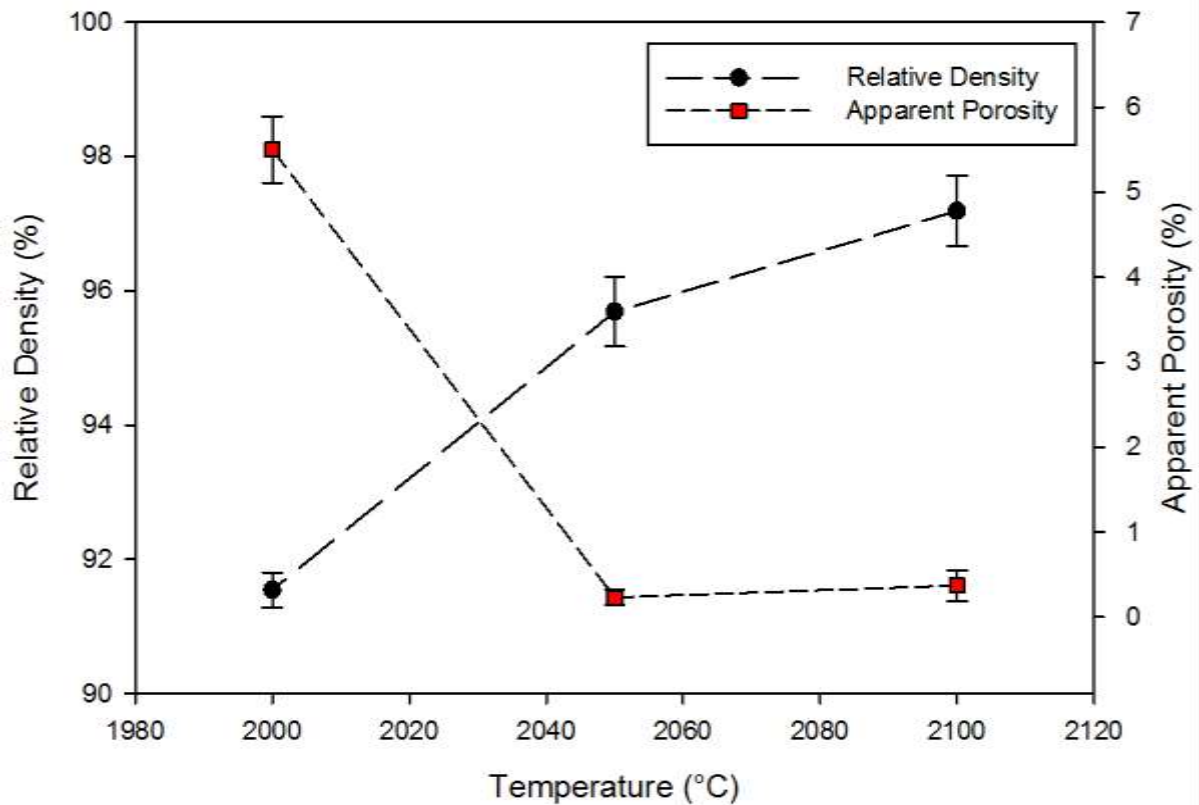


Figure 35. Density and porosity plot as a function of sintering temperature

Table IX shows the average and standard deviations for the density data

Table IX. Average Relative Density and Standard Deviation

Temperature (°C)	Average Relative Density (g/cc)	Standard Deviation
2100	97.19	0.52
2050	95.69	0.52
2000	91.54	0.26

The ANOVA results for the three sintering temperatures showed that none of the variables were significant. Samples fired at 2100°C showed that model was not significant however, that dwell temperature had the most effect on the results, although not statistically significant (Table X). Samples fired at 2050°C and 2000°C showed that the means were a better representation of the data than the models.

Table X. ANOVA Results for Relative Density (2100°C) Response

Source	Sum of Squares	Df	Mean Square	F Value	p-value (Prob>F)	
Model	1.01	1	1.01	4.21	0.0581	<i>Not Significant</i>
<i>Dwell Temperature</i>	1.01	1	1.01	4.21	0.0581	
Residual	3.59	15	0.24			
<i>Lack of Fit</i>	2.38	11	0.22	0.71	0.7041	<i>Not Significant</i>
<i>Pure Error</i>	1.21	4	0.3			
Cor. Total	4.6	16				

Figure 36 is a contour plot of the 2100°C relative density response data. It shows the surface the model follows to optimize the response with flow rate and dwell temperature with relative density values on the contour lines. The plot shows that a low dwell temperature with any

flow rate will yield an increased relative density. The atmosphere variable was removed from the model because it had no effect; the value was set to 5 % O₂ for this plot.

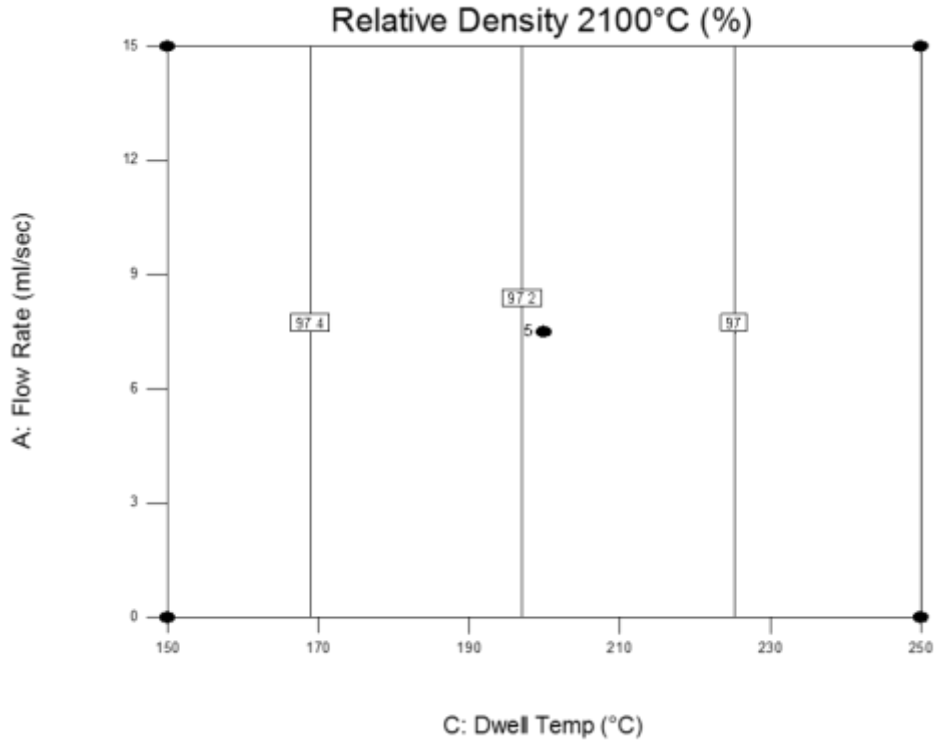


Figure 36. Contour plot for relative density (2100°C)

Micrographs were taken of the best performing samples (those with the highest density, lowest weight loss and highest carbon content) for each sintering temperature. Figure 37 shows the progression of the microstructure with increasing sintering temperature. The bottom row is images of the same region as the top row, just at a higher magnification. All the micrographs are secondary electron images as to try and differentiate porosity from the darker gray domains (boron and carbon rich zones). The samples were not etched.

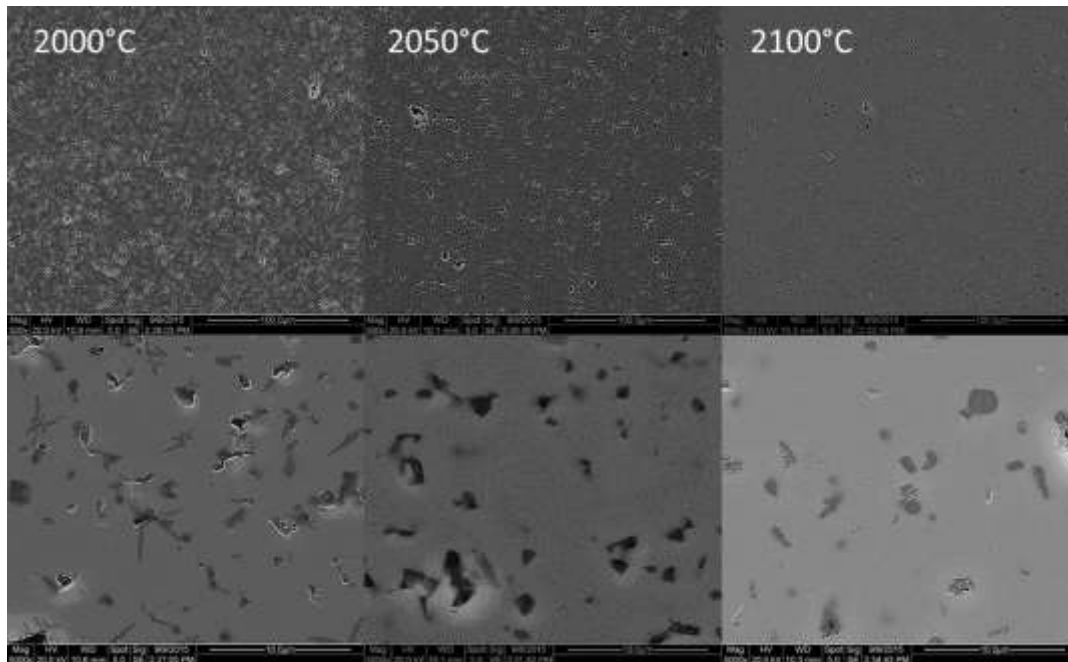


Figure 37. Micrographs of polished sintered samples

B.2 Response: Mass Loss

The ANOVA results, Table XI, shows that the linear model is significant (having a p-value less than 0.0500) although it had to reduce it by removing atmosphere, dwell temperature and their first order interactions. Flow rate was considered to be significant. Lack of fit was ruled not significant, which is good because the model fits.

Table XI. ANOVA Results for Mass Loss Response

Source	Sum of Squares	Df	Mean Square	F Value	p-value (Prob>F)	
Model	0.018	1	0.018	6.49	0.0223	<i>Significant</i>
<i>Flow Rate</i>	0.018	1	0.018	6.49	0.0223	
Residual	0.042	15	2.783E-003			
<i>Lack of Fit</i>	0.013	11	1.165E-003	.16	0.9927	<i>Not Significant</i>
<i>Pure Error</i>	0.029	4	7.230E-003			

Cor. Total	0.06	16				
------------	------	----	--	--	--	--

The contour plot for mass loss can be seen in Figure 38. The axis for this plot is atmosphere and flow rate. It shows a dependence only on flow rate, a low flow rate resulted in minimal weight loss. These results were independent from changes in atmosphere and dwell temperature. The dwell temperature used in this plot was 200°C.

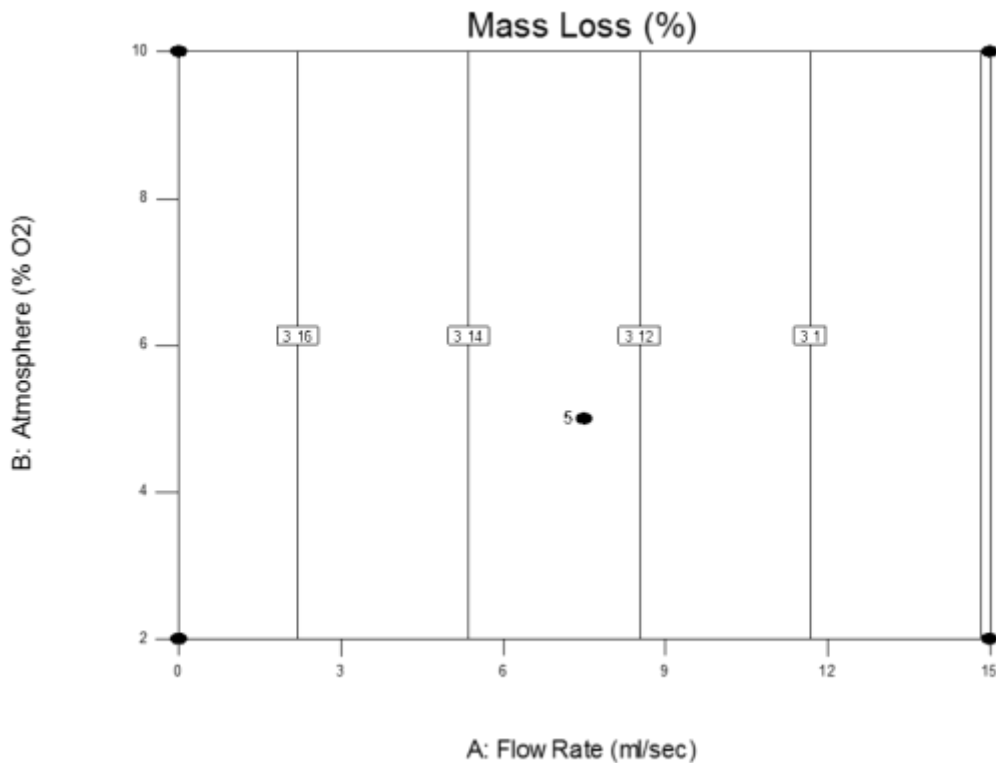


Figure 38. Contour plot for mass loss

B.3 Response: LECO Carbon Analysis

LECO free carbon analysis yielded questionable results. The results showed all samples being near or below the lower detection limit (0.02 wt. %) for free carbon content. This raised questions because of the high sintering performances of all samples.

It has been reported that SiO₂ will inhibit the sintering of boron doped SiC.^{13,14,15} The SiO₂ is present as a surface layer on the SiC grains. This layer alters the sinterability by acting as a

surface contaminant therefore decreasing the surface energy.^{14,15} The free carbon acts to reduce the surface silica layer, therefore increasing surface energy and sinterability.

The samples densified when heat treated and carbon domains can be found in the microstructure. If the LECO results are correct, we would expect to see dramatically lower densities, higher porosities and no carbon in the microstructure.

The amount of silica present in the starting SiC powder was calculated by a LECO oxygen analysis (data obtained from Nikolas Ninos, Calix Ceramic Solutions, Clarence, NY). Table XII shows the results from these calculations. This allowed for a more accurate chemistry to be calculated from the true density method. From these calculations, the amount of carbon needed to reduce the silica was calculated, 0.62 weight percent. This did not account for carbon introduced with the starting materials.

Table XII. Starting SiC Powder Chemistry from LECO Oxygen Results

Density for Carbon (g/cc)	Material (wt. %)	Percentage (wt. %)
	<i>O2 measured</i>	<i>0.17</i>
Measured: 1.706	SiC	97.61
	SiO ₂	1.03
	C	1.36
	Total	100
	C needed	-0.74

After adjusting for the carbon introduced with the starting SiC material, -0.74 weight percent of carbon is needed. Meaning that there is enough free carbon in the starting material to reduce the silica and still have 0.74 wt. % excess carbon. After the B₄C is added, the amount of excess carbon needed is 0.77 wt. % (see chemistries in Table VI).

The LECO results stated that the free carbon content in the pyrolyzed samples was less than 0.02 weight percent. Assuming pyrolysis yielded no carbon; the amount introduced by the starting

materials (1.39 wt. %) is well above the lower detection limit (0.02 wt. %) and should have been identified.

If the LECO test results are correct, all of the samples are extremely deficient in the free carbon needed to reduce the silica. From this and the high sinterability of the samples, it is reasonable to question if LECO free carbon analysis is the optimal method to quantify carbon for this application. Because of the questionability of the test, LECO free carbon analysis was removed as a response to the S.E.D.

B.4 Response: Carbon Content via True Density

In order to quantify the carbon content attained from pyrolysis, mineralogy was determined via helium pycnometry measurements. It has been shown that phase composition can be accurately (within 5% error) quantified via the rule of mixtures and intrinsic property measurements.²⁴

The material in this work is a binary system, “carbide” and carbon. Therefore, measuring density is the only measurement needed to calculate the quantity of the different phase compositions. The carbide is the mixture of SiC and B₄C. It is added as a constant ratio of each other, allowing it to be treated as one material with a composite density.

By measuring density and using the rule of mixtures, the volume fraction of carbon can be calculated for the raw SiC, B₄C and overall system. Calculating the amount of carbon in the starting materials allows the total free carbon percent to be corrected, yielding only the free carbon obtained from polymer pyrolysis. It is important to note that these calculations yield volume percent, a conversion to weight percent is necessary.

The ANOVA results show that the model represents the data well (Table XIII). Both the model and flow rate were found to be significant. Model reduction removed both atmosphere and dwell temperature and the lack of fit test showed to not be significant (which is desired).

Table XIII. ANOVA Results for Carbon Content Response

Source	Sum of Squares	Df	Mean Square	F Value	p-value (Prob>F)	
Model	56.71	1	56.71	7.71	0.0141	<i>Significant</i>
<i>Flow Rate</i>	56.71	1	56.71	7.71	0.0141	

Residual	110.34	15	7.36			
<i>Lack of Fit</i>	40.16	11	3.65	0.21	0.9827	<i>Not Significant</i>
<i>Pure Error</i>	70.18	4	17.54			
Cor. Total	167.05	16				

The contour plot for carbon yield is seen in Figure 39. The only significant variable was flow rate therefore; the plot shows that a high flow rate resulted in high carbon content. Atmosphere and dwell temperature were insignificant in this model, dwell temperature was set to 200°C for this plot.

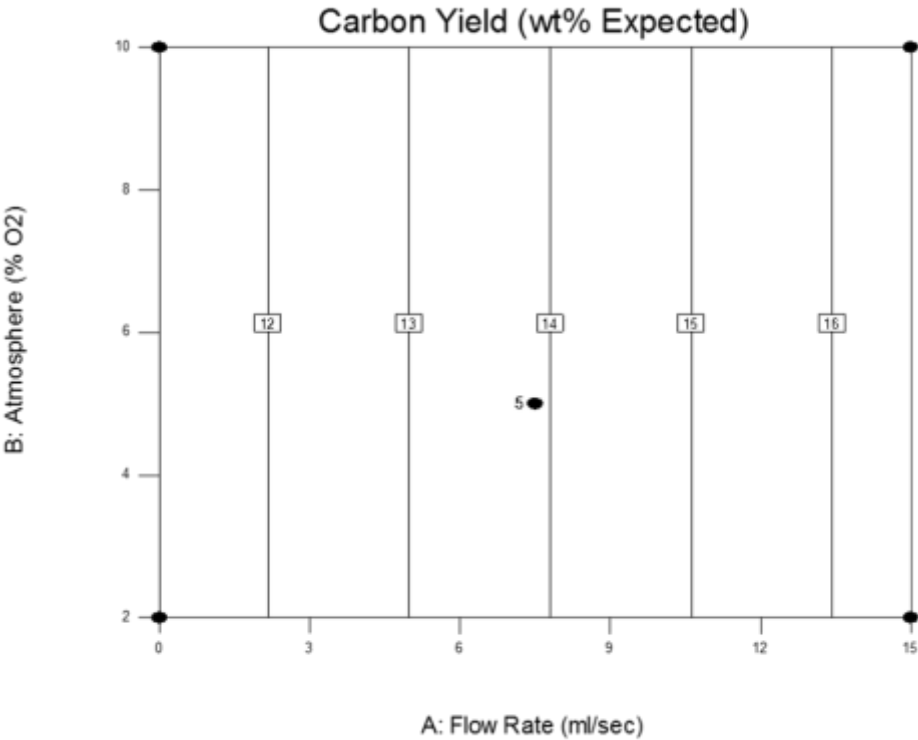


Figure 39. Contour plot for carbon yield

B.5 Optimization

Weights can be assigned to the different responses so that they can influence the model for optimization. Carbon content was given the highest weight followed by the relative densities and lastly, weight loss. This allows the program to calculate the optimal conditions to satisfy the requirements of the responses. Maximum carbon content, maximum density and minimal weight loss is desirable. The program displays the results of the optimization as a desirability plot on a scale 0-1, 1 being most desirable. Figure 40 is a contour plot of desirability for the proposed pyrolysis optimization model.

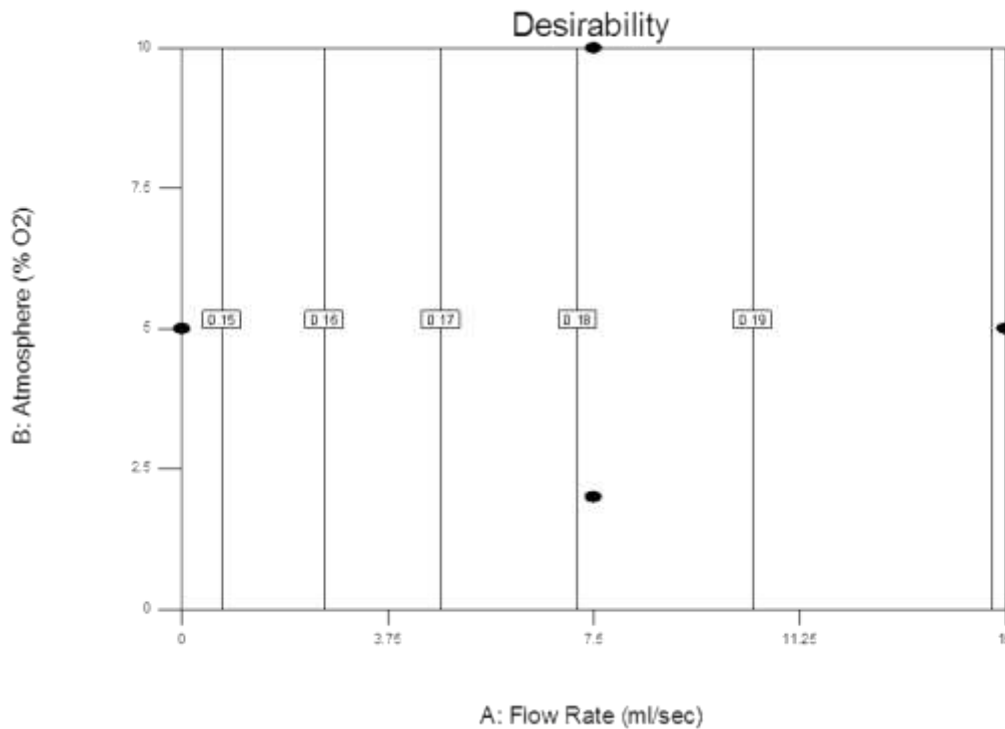


Figure 40. Contour plot of desirability for pyrolysis process optimization

Figure 41 is a cube plot of desirability; it is similar to Figure 9, the design matrix plot. This shows the desirability as a function of the three factors. Although dwell temperature was not significant, this plot shows that a low dwell temperature coupled with a high flow rate is most desirable, regardless of atmosphere. The points circled in red are the points in the design with the highest desirability.

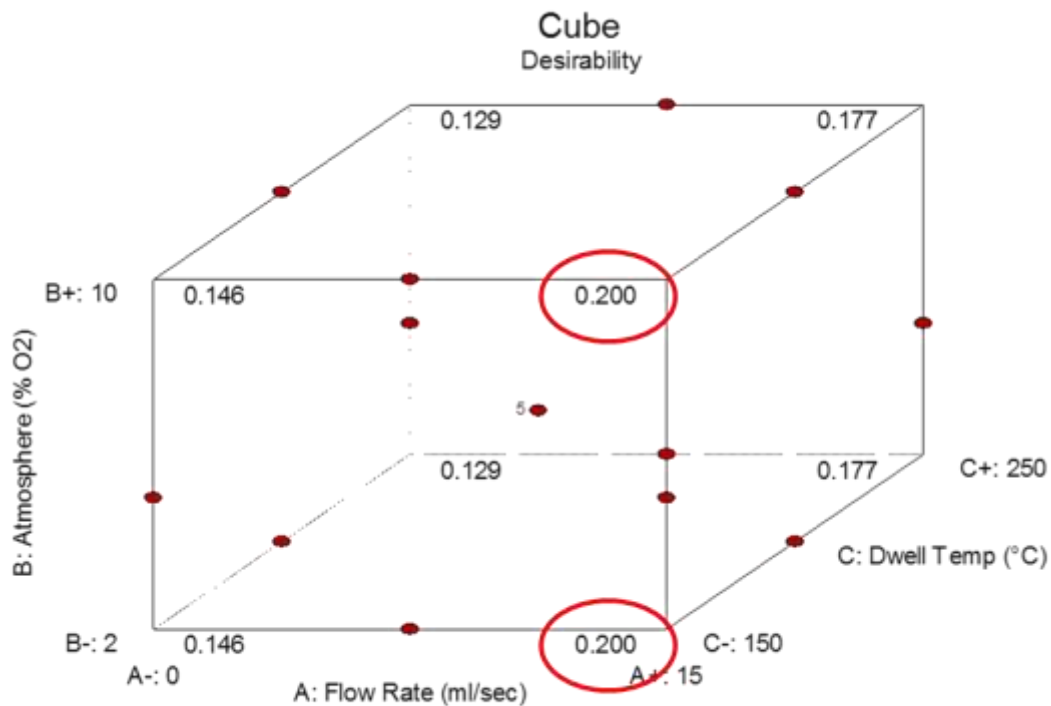


Figure 41. Cube plot of desirability

Optimization was calculated based off of the models fit to the responses, their statistical significances and the weights allocated to the responses. In doing this an empirical model is created to predict the values of the responses given a specific set of pyrolysis parameters. Table XIV shows the factors and their optimal levels. 5% O₂ was chosen because it is in the middle of the range, recall that it is not a statistically significant variable.

Table XIV. Table of Optimization Parameters

<i>Factor</i>	<i>Level</i>
Flow Rate (ml/sec)	15
Atmosphere (% O ₂)	5
Dwell Temperature (°C)	150

V. SUMMARY AND CONCLUSIONS

Maximizing carbon yield from the pyrolysis of phenolic resin in a SiC matrix was studied. The hypothesis of increasing carbon yield by selectively stripping hydrogen from the cured polymer structure was supported.

The TGA data for both the paraffin and phenolic samples supports the hydrogen stripping hypothesis. Paraffin shows that a low dwell temperature (below 175°C) coupled with high oxygen levels (21.5% O₂) results in a high carbon yield. If the dwell temperature is increased and oxygen level decreased the yield drops, suggesting that the polymer remains saturated and depolymerizes. The phenolic samples are consistent in showing that low dwell temperatures (200°C) result in the highest yield. Also, it is evident that there is a contribution from the oxygen level. It shows that 5% O₂ results in the highest carbon yield, when compared to 2% and 21.5% O₂. Suggesting that having oxygen in the gas helps to increase the carbon yield.

The S.E.D. showed that the flow rate of the gas has a statistically significant interaction with the outcome of the pyrolysis. Increasing the flow rate increases both the carbon yield and sintered density, along with lowering the weight loss from pyrolysis. The dwell temperature was shown not to be significant however it influenced the sintered density at 2100°C. The atmosphere (O₂ level) was found to be insignificant to all responses.

The carbon yields from these tests were lower than the yields obtained from the standard pyrolysis. However, the data suggests that the mass loss is not complete when pyrolyzing using the standard cycle.

VI. FUTURE WORK

Adjusting the standard pyrolysis cycle to a peak temperature of 750°C should be tested. This will allow the results from the S.E.D. to be compared directly to the standard pyrolysis results.

Partial pyrolysis runs of paraffin and phenolic resin that are stopped after the dwell should be tested. These tests should be done with low dwell temperatures and an oxidative environment. Analyzing the material using FTIR or Raman spectroscopy should be done to understand the bonding environments of the polymers, post (partial) pyrolysis. These results can help to understand how much hydrogen is being removed and what the resulting polymer structure looks like.

Expanding the experimental matrix to include nitrogen should be tested. This can be done with a separate S.E.D. that is designed with nitrogen and a slightly oxidative environment to depict the differences. This experiment should be done with a fixed flow rate (as high as the system allows) and with a dwell temperature of 150°C. In doing this, the only variable that is tested is the atmosphere and it will statistically confirm what gas chemistry is optimal for this process.

Once the optimal atmosphere is confirmed, tests should be done on varying sample volumes. In industry, parts of a wide volume range are produced. These tests will confirm that the pyrolysis model is scalable.

It is known that having excess carbon in sintered SiC can change the electrical and mechanical properties of the material. Even though the samples in this work did not yield more carbon than the standard pyrolysis cycle, they sintered very well. Samples prepared from both the standard pyrolysis and the “optimized” pyrolysis cycles should be tested for electrical conductivity and strength. A free carbon limit can be established from these tests.

The optimal conditions to retain carbon during pyrolysis were found (within the tested matrix). It would be worthwhile for binder burnout studies to use this information on carbon retention to understand how to remove it efficiently.

REFERENCES

- 1 J. Wang, H. Jiang, and N. Jiang, "Study on the pyrolysis of phenol-formaldehyde (PF) resin and modified PF resin," *Thermochim. Acta*, **496** [1-2] 136–142 (2009).
- 2 K.A. Trick and T.E. Saliba, "Mechanisms of the Pyrolysis of Phenolic Resin in a Carbon/Phenolic Composite," *Carbon*, **33** [11] 1509–1515 (1995).
- 3 H. Jiang, J. Wang, S. Wu, Z. Yuan, Z. Hu, R. Wu, and Q. Liu, "The pyrolysis mechanism of phenol formaldehyde resin," *Polym. Degrad. Stab.*, **97** [8] 1527–1533 (2012).
- 4 G. Raffin, B. Salino, and O. Pai, "Phenolic resins Part 6 . Identifications of volatile organic molecules during thermal treatment of neat resols and resol filled with glass fibers," *Polymer*, **41** [19] 7123–7132 (2000).
- 5 M. Sobera and J. Hetper, "Pyrolysis -gas chromatography- mass spectrometry of cured phenolic resins," *J. Chromatogr. A*, **993** [1-2] 131–135 (2003).
- 6 C. Chang and J.R. Tackett, "Characterization of Phenolic Resins with Thermogravimetric-Mass Spectrometry," *Thermochim. Acta*, **192** 181–190 (1991).
- 7 M. Lucarini, P. Pedrielli, G.F. Pedulli, S. Cabiddu, and C. Fattuoni, "Bond Dissociation Energies of O–H Bonds in Substituted Phenols from Equilibration Studies," *J. Org. Chem.*, **61** [2] 9259–9263 (1996).
- 8 G. da Silva, C.-C. Chen, and J.W. Bozzelli, "Bond dissociation energy of the phenol OH bond from ab initio calculations," *Chem. Phys. Lett.*, **424** [1-3] 42–45 (2006).
- 9 C. Barckholtz, T. a. Barckholtz, and C.M. Hadad, "C-H and N-H bond dissociation energies of small aromatic hydrocarbons," *J. Am. Chem. Soc.*, **121** [2] 491–500 (1999).
- 10 S.J. Blanksby and G.B. Ellison, "Bond dissociation energies of organic molecules," *Acc. Chem. Res.*, **36** [36] 255–263 (2003).
- 11 H. Lee and W.M. Carty, Alfred University, Alfred, NY, June-2013-September 2015, Private Communication.
- 12 D.R. Gaskell, *Introduction to the Thermodynamics of Materials*, 5th ed. Taylor & Francis Inc., 2008.
- 13 S. Prochazka and R.M. Scanlan, "Effect of Boron and Carbon on Sintering of SiC," *J. Am. Ceram. Soc.*, **58** [1-2] 72 (1975).
- 14 S. Prochazka, "The Role of Boron and Carbon in the Sintering of Silicon Carbide.;" pp. 171–179 in *Symp. Spec. Ceram. 6*. Schenectady, NY, 1975.

- 15 E. Gugel, "On the Sintering of Silicon Carbide," *Ceram. Forum Int.*, **62** [2] 89–91 (1985).
- 16 N. Ninos, Alfred University, Alfred, NY, June 2014–September 2015, Private Communication.
- 17 P.L.A. Knoop Andre, *Phenolic Resins*. Springer-Verlag, Berlin, 1985.
- 18 H. Jiang, J. Wang, S. Wu, B. Wang, and Z. Wang, "Pyrolysis kinetics of phenol-formaldehyde resin by non-isothermal thermogravimetry," *Carbon*, **48** [2] 352–358 (2010).
- 19 L. Costa and E.M. Pearceb, "Structure-charring relationship in phenol-formaldehyde type resins," *Polym. Degrad. Stab.*, **56** [1] 23–35 (1997).
- 20 G.F. Sykes, Decomposition "Characteristics of A Char-Forming Phenolic Polymer Used for Ablative Composites," NASA TN D-3810, Langley Research Center, Langley Station Hampton, VA, 1967.
- 21 K.A. Trick, T.E. Saliba, and S.S. Sandhu, "A kinetic model of the pyrolysis of phenolic resin in a carbon/phenolic composite," *Carbon*, **35** [3] 393–401 (1997).
- 22 M. Blazsó and T. Tóth, "Thermal decomposition of methylene bridges and methyl groups at aromatic rings in phenol-formaldehyde polycondensates," *J. Anal. Appl. Pyrolysis*, **10** [1] 41–50 (1986).
- 23 K. Heartline, LECO, St. Joseph, MI, May 2015, Private Communication.
- 24 K. Tseng, H. Lee, and W.M. Carty, "A Potential Short-Cut to Quantitative Mineralogy," pp. 40–53 in *Am. Ceram. Soc. St. Louis Sect. Refract. Ceram. Div.* St. Louis, 2015.
- 25 "Standard Test Methods for Apparent Porosity, Water Absorption, Apparent Specific Gravity, and Bulk Density of Burned Refractory Brick and Shapes by Boiling Water," ASTM Subcommittee C08.03. American Society of Testing and Materials, West Conshohocken, PA.
- 26 M. Freund, R. Csikos, S. Keszthelyi, and G.Y. Mozes, *Parrafin Products*. 1982.
- 27 H. Marsh and R. Menendez, "Chapter 2 Mechanisms of Formation of Isotropic and Anisotropic Carbons," pp. 37–70 in *Introd. to carbon Sci.* 1989.

APPENDIX

A. S.E.D. Data

		Factor 1	Factor 2	Factor 3	Response 1	Response 2	Response 3	Response 4	Response 5
Std	Run	A:Flow Rate	B:Atmosphere	C:Dwell Temp	Relative Density 2100C	Relative Density 2050C	Relative Density 2000 C	Mass Loss	Carbon Yield
		ml/sec	% O2	C	%	%	%	%	wt% Expected
12	1	7.5	10	250	97.18	95.87	91.75	3.14	13.12
10	2	7.5	10	150	97.17	95.81	91.92	3.15	14.83
3	3	0	10	200	97.67	95.42	91.58	3.15	14.97
4	4	15	10	200	97.46	95.96	91.57	3.1	19.35
16	5	7.5	5	200	96.01	95.76	91.37	3.02	16.52
8	6	15	5	250	96.31	95.03	91.51	3.02	15.57
6	7	15	5	150	97.57	95.7	91.49	3.08	18.25
15	8	7.5	5	200	97.27	95.5	91.49	3.07	18.23
13	9	7.5	5	200	96.65	95.87	91.81	3.17	9.63
7	10	0	5	250	97.61	95.63	91.65	3.15	9.25
17	11	7.5	5	200	97.22	95.67	90.98	3.22	8.66
5	12	0	5	150	97.95	96.01	92.01	3.21	10.87
14	13	7.5	5	200	97.25	95.69	91.54	3.19	14.06
1	14	0	2	200	96.86	95.23	91.28	3.19	11.03
9	15	7.5	2	150	97.96	95.9	91.72	3.09	14.93
11	16	7.5	2	250	96.71	96.08	91.25	3.08	12.69
2	17	15	2	200	97.2	95.62	91.65	3.12	14.25

“Never for money, always for love, cover up and say goodnight.”

-David Byrne